END
FILMED
3 92
DTIC

MICROCOPY RESOLUTION TEST CHART

NATIONAL BUREAU OF STANDARDS-1963-A

AD-A247 093

DTIC

R92-928101

Theoretical Studies of the Electronic and Resonance Structure of Atomic and Molecular Negative Ions
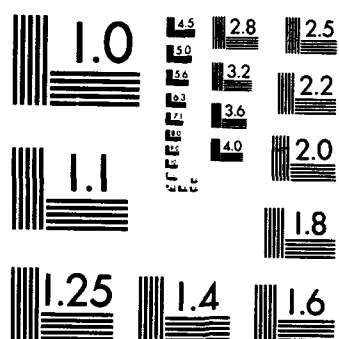
UNITED
TECHNOLOGIES
RESEARCH
CENTER

UNITED TECHNOLOGIES RESEARCH CENTER

East Hartford, Connecticut 06108

**UNITED
TECHNOLOGIES
RESEARCH
CENTER**

East Hartford, Connecticut 06108

R92-928101

Theoretical Studies of the Electronic and Resonance Structure of Atomic and Molecular Negative Ions

Final Technical Report

January 1992

Contract No. F49620-89-C-0019
Project Task 2301/A7

H. H. Michels
J. A. Montgomery, Jr.

92-05585

92 3 03 058

AEOSR-TR- ᵓ2 ᵥ₀ 16

REPORT DOCUMENTATION PAGE		Form Approved OMB No. 0704-0188
1a. REPORT SECURITY CLASSIFICATION Unclassified	**1b. RESTRICTIVE MARKINGS**	
2a. SECURITY CLASSIFICATION AUTHORITY	**3. DISTRIBUTION/AVAILABILITY OF REPORT** Approved for public release; distribution unlimited.	
2b. DECLASSIFICATION/DOWNGRADING SCHEDULE		
4. PERFORMING ORGANIZATION REPORT NUMBER(S) R92-928101	**5. MONITORING ORGANIZATION REPORT NUMBER(S)**	

6a. NAME OF PERFORMING ORGANIZATION United Technologies Research Center	6b. OFFICE SYMBOL (If applicable)	7a. NAME OF MONITORING ORGANIZATION Defense Plant Representative Office
6c. ADDRESS (City, State, and ZIP Code) Silver Lane East Hartford, CT 06108		7b. ADDRESS (City, State, and ZIP Code) DPRO Pratt & Whitney East Hartford, CT 06108
8a. NAME OF FUNDING/SPONSORING ORGANIZATION Air Force Office of Scientific Research	8b. OFFICE SYMBOL (If applicable) *AFOS NE*	9. PROCUREMENT INSTRUMENT IDENTIFICATION NUMBER F49620-89-C-0019

8c. ADDRESS (City, State, and ZIP Code) Bolling Air Force Base Washington, D.C. 20332	10. SOURCE OF FUNDING NUMBERS			
	PROGRAM ELEMENT NO. *61103F*	PROJECT NO. 2301	TASK NO. *A7*	WORK UNIT ACCESSION NO

11. TITLE (Include Security Classification)

Theoretical Studies of the Electronic and Resonance Structure of Atomic and Molecular Negative Ions

12. PERSONAL AUTHOR(S)

Michels, H. Harvey

13a. TYPE OF REPORT Final Report	13b. TIME COVERED FROM 11/15/88 TO 11/15/91	14. DATE OF REPORT (Year, Month, Day) January 1992	15. PAGE COUNT 78

16. SUPPLEMENTARY NOTATION

17. COSATI CODES			18. SUBJECT TERMS (Continue on reverse if necessary and identify by block number)
FIELD	GROUP	SUB-GROUP	potential energy surfaces, H^-, Li_2, ion-molecule reactions, negative ions, H_2, Li_2^-, dissociation attachment, H_3^-

19. ABSTRACT (Continue on reverse if necessary and identify by block number)

This technical program constitutes a theoretical research investigation of the electronic structure of atomic and molecular ions and of radiative and collisional processes describing their formation and/or destruction. This study is directed toward elucidating the structure of both thermodynamically stable cations and anions, and resonance or metastable excited states in such systems. In addition, this study will include an analysis of the effects of both static E-fields and time dependent laser fields on resonance excitation, stimulated autodetachment and radiative electron attachment processes in negative ion systems and ion-pair production in Rydberg atom collisions. The goals of this research program are to develop accurate computational techniques which are applicable to studies of the electronic structure and radiative properties of small atomic and molecular ions and to carry out detailed calculations of the structure of several prototype species, including light element alkalis, alkaline earths and the noble gases. It is anticipated that the results of this program will furnish fundamental data and provide a better understanding of several detailed experimental studies that are currently in progress in this area, including work at SRI and ORNL. Areas of application of this research work include thermonuclear reactor programs, neutral and negative ion particle beam source development, high current switching devices and discharge plasma devices.

20. DISTRIBUTION/AVAILABILITY OF ABSTRACT ☐ UNCLASSIFIED/UNLIMITED ☒ SAME AS RPT. ☐ DTIC USERS	21. ABSTRACT SECURITY CLASSIFICATION Unclassified	
22a. NAME OF RESPONSIBLE INDIVIDUAL Dr. Robert Barker	22b. TELEPHONE (Include Area Code) (202)767-4908	22c. OFFICE SYMBOL NE

DD Form 1473, JUN 86 Previous editions are obsolete. SECURITY CLASSIFICATION OF THIS PAGE

Unclassified

i

FOREWORD

This report was prepared for the Air Force Office of Scientific Research, United States Air Force by the United Technologies Corporation, Research Center, East Hartford, Connecticut, under Contract F49620-89-C-0019, Project-Task No. 2301/A7. The performance period for the technical program was from 15 November 1988 through 14 November 1991. The project monitor was Lt. Colonel James A. Lupo, USAF.

ACKNOWLEDGEMENTS

R92–928101

Theoretical Studies of the Electronic and Resonance Structure of Atomic and Molecular Negative Ions

TABLE OF CONTENTS

TABLE OF CONTENTS (continued)

LIST OF TABLES

LIST OF FIGURES

R92-928101

Theoretical Studies of the Electronic and Resonance Structure of Atomic and Molecular Negative Ions

ABSTRACT

This technical program constitutes a theoretical research investigation of the electronic structure of atomic and molecular ions and of radiative and collisional processes describing their formation and/or destruction. This study is directed toward elucidating the structure of both thermodynamically stable cations and anions, and resonance or metastable excited states in such systems. In addition, this study will include an analysis of the effects of both static E-fields and time dependent laser fields on resonance excitation, stimulated autodetachment and radiative electron attachment processes in negative ion systems and ion-pair production in Rydberg atom collisions. The goals of this research program are to develop accurate computational techniques which are applicable to studies of the electronic structure and radiative properties of small atomic and molecular ions and to carry out detailed calculations of the structure of several prototype species, including light element alkalis, alkaline earths and the noble gases. It is anticipated that the results of this program will furnish fundamental data and provide a better understanding of several detailed experimental studies that are currently in progress in this area, including work at SRI and ORNL. Areas of application of this research work include thermonuclear reactor programs, neutral and negative ion particle beam source development, high current switching devices and discharge plasma devices.

STATEMENT OF WORK
for
Contract F49620-89-C-0019

The Contractor shall conduct a theoretical research investigation of the electronic structure of atomic and molecular ions and of the radiative and collisional mechanisms describing their formation and/or destruction. This investigation shall include *ab initio* calculations of atomic and molecular electronic structures, an analysis of resonance excitation and metastable states, stimulated autodetachment and radiative electron attachment processes in prototype ion systems, and studies of ion-pair production from the collisions of Rydberg atoms. Experimental data collected at ORNL, LANL, SRI and other sites where there are on-going studies of negative ion sources, shall be iteratively examined and integrated with the results generated by this theoretical investigation. This investigation shall be carried out with *ab initio* methods using electronic structure, radiative property and collisional cross-section codes that have previously been developed at this Center, including such modifications as are necessary to implement laser field effects. Specifically, this investigation shall comprise the following:

1. Quantum mechanical calculations of the electronic structure, potential energy surfaces (for molecular species) and resonance positions and widths for positive and negative atomic and molecular ions. These calculations shall be carried out for species to be chosen from the first and second row atomic ions. Heavier alkali ions may also be included. The choice of species to be studied shall be directed in part by on-going parallel experimental efforts at ORNL, LANL, SRI, as well as several university laboratories.

2. Variational R-matrix calculations of resonance states excited through electron-molecule collisions.

3. Quantum mechanical calculations of resonance excitation and analysis of laser stimulated electron attachment and detachment processes in negative ion systems. These calculations shall include studies of Li^-, Na^- and He_2^-.

4. Analysis of ion-pair formation in thermal energy Rydberg atom collisions. Both alkali and alkali/noble gas systems shall be examined to provide interpretations of the experimental studies at SRI and AVCO on these systems.

BACKGROUND

Recent successes in the tokamak program and in other controlled thermonuclear research programs (Ref. 1) have focused attention on the problem of developing an efficient high–energy particle beam source. For several applications, a neutral beam with energies above 200 meV is desired. The acceleration of negative ions to such energies, followed by neutralization through a stripping reaction, appears at the present time to be the most efficient approach for producing a high energy neutral particle beam.

In another area, the feasibility of particle beams (both charged and neutral) as military defense weapons has been under study. The proposed endoatmospheric applications require high intensity sources and mainly focus on the problems of beam stability and propagation characteristics. Exoatmospheric applications require lower intensity sources but of very high quality. Design goals are highly collimated beams with a narrow energy spread.

A magnetron–type negative H^- source has been reported by Belchenko, Dimov and Dudnikov (BDD) (Ref. 2) that has produced H^- current densities of several A cm^{-2}. This device operates as a plasma discharge in an atmosphere of hydrogen gas with cesium or other alkalis present at $\sim$ 0.01 percent. The mechanism for the production of H^- was believed to involve a catalyzed surface reaction whereby H^- ions are produced by transfer of electrons from Cs atoms that are adsorbed on the cathode surface (Refs. 3, 4). The detailed kinetic mechanisms of such surface reactions are still uncertain and parametric experimental studies are currently underway at LANL, LBL, IRT and at other laboratories to elucidate the mechanisms and operating characteristics of BDD and similar devices and to develop information for their scale–up to higher current densities. Diagnostics of H^- source devices are also underway at Brookhaven (Ref. 5) using beam probe and spectroscopic techniques.

Concurrent with these surface–plasma reactions are several electron–H_2/H volume–dependent processes that may lead either to the production of H^- or, in reverse, may act as important destructive processes of the negative ions after they are formed. Photodetachment experiments by Bacal and Hamilton (Ref. 6) in hydrogen plasmas indicate H^- densities 100 times larger than that predicted from simple electron attachment mechanisms. Further, these experiments indicate a nonlinear dependence of the production of H^- on electron density, at least for densities less than 10^{10} cm^{-3}. Several mechanisms (Ref. 7) have been proposed to explain these volume–dependent H^- production processes but the cross–sections for many of the reactions leading to H^- are uncertain.

In addition to studies of thermodynamically stable negative ions, there has been recent interest in the metastable or resonant states in these systems. Compound states of atomic negative

3

ions have been a subject of interest in atomic physics for over forty years. The first observation of a compound negative ion state was the detection of long-lived He^- ions in a mass spectrometer by Hiby (Ref. 8) in 1939. Holoien and Midtdal (Ref. 9) theoretically showed that He^- $(1s2s2p)^4P°$ was stable relative to $He(1s2s)^3S$ and thereby offered an explanation of Hiby's observation of long-lived He^- ions. In 1963, Schulz (Ref. 10) reported evidence for a scattering resonance in He at $\sim$ 19.3 eV which was attributed to $He^-(1s2s^2)^2S$. This was the first experimental observation of an electron scattering resonance in an atomic system. Since that time, compound states of atoms have been seen in many elastic and inelastic channels in electron–atom scattering (Ref. 11), in ion–atom scattering cross sections (Ref. 12), in laser photodetachment cross sections (Ref. 13), and in dissociative electron attachment studies (Refs. 14, 15). Compound states of doubly charged negative ions have also been detected (Ref. 16).

The spectroscopy of metastable negative ions has been the subject of several experimental and theoretical investigations (Refs. 17–21). Although much attention has been given to the problem of atomic anion formation, more recent studies have examined diatomic anions, especially those of the lighter elements (Refs. 22–25). In a recent study (Ref. 23), the electronic structure of the newly discovered (Ref. 22) metastable He_2^- ion was examined using CI wavefunctions. This study indicated that only the $^4\Pi_g$ state of He_2^- was metastable relative to $He_2\ [a^3\Sigma_u^+] + e$. More recently, by double charge exchange of He_2^+ ions in lithium vapor, Kvale, et al. (Ref. 26) have examined the autodetachment spectrum for $^4He_2^-$ and $^3He_2^-$ ions and have observed two autodetachment peaks. The first (low–energy) peak was identified as autodetachment from the first vibrational level of He_2^- $[^4\Pi_g]$ to $He_2\ [a^3\Sigma_u^+] + e$ and the second as autodetachment to the $He_2\ [X^1\Sigma_g^+] + e$ repulsive continuum, similar to that observed by Bae, et al. (Ref. 22).

The coupling of this experimental data to theoretical studies of the electronic structure of the He_2^- anion has yielded a good understanding of the spectroscopy of this system. Because of the difficulties in conducting experiments to measure kinetic processes in these metastable and compound ion systems, the development of sound theoretical methods for calculating the positions and widths from analysis of their electronic structure appears desirable. In this direction, we have undertaken a series of calculations for the $He/He^-/He_2^-$ and $Li/Li^-/Li_2^-$ systems in an effort to understand their resonance structure.

The calculations for the He^-/He_2^- system were carried out to gain a better understanding of the experiments of Bae, Coggiola and Peterson (Ref. 22), who were the first to report observations

of the metastable He_2^- ion, and the more recent autodetachment experiments reported by Kvale, et al. (Ref. 26) for this system. Our results show that only the lowest $^4\Pi_g$ of He_2^- is metastable relative to $He_2 [a^3\Sigma_u^+] + e$ and that the lowest lying $^4\Pi_u$, $^4\Sigma_g^+$ and $^4\Sigma_u^+$ states are all autoionizing. However since the $^4\Pi_{5/2g}$ spin–orbit state has a long (~ 400 μ sec) lifetime, it should be possible to laser induce transitions from this level to the upper resonant negative ion states. Such an experiment, using a tunable laser, is now under development by Compton and co–workers at Oak Ridge National Laboratory. A complimentary experiment would involve the possible production of thermodynamically stable negative ions by stimulated radiative attachment of electrons to neutral atoms or molecules. An alkali system would appear to be a good choice for such studies since both Li^- and Li_2^- are stable and exhibit an electronic structure which includes resonances that could be reached by conventional tunable lasers.

In a related area, there is now considerable interest in understanding ion–pair production in low energy collisions of Rydberg atoms. Ciocca, et al. (Ref. 27) and Cheret and Barbier (Ref. 28) have reported efficient ion–pair formation in laser excited alkali systems. In contrast, McGeoch and Schlier (Ref. 29) find no ion–pair production, as a primary process, in thermal energy collisions between lithium Rydberg atoms. Conventional curve–crossing mechanisms are not capable of explaining these results and new theoretical developments are needed. An experiment to study ion–pair formation in the reaction of $He(^3S)$ atoms and alkali Rydberg atoms has been suggested by Peterson (SRI). This system would be an ideal candidate for a collaborative experimental and theoretical study of the mechanism of ion–pair production.

The goals of this research program were to identify the electronic and resonance structure of atomic and molecular positive and negative ions, to study the effects of high laser fields on stimulated autodetachment and radiative electron attachment in such systems, and to carry out theoretical studies of atomic Rydberg state interactions leading to ion–pair production. This theoretical research effort was developed to compliment the experimental studies of ion formation processes that are being carried out by Peterson and co–workers (SRI), by McGeoch (AVCO) and by several European research groups.

RESEARCH PROGRESS

1. Electronic Structure and Autodetachment Studies of Molecular Negative Ions

During the past several years, we have undertaken a series of calculations of Li_2^- in order to assess the energetics of this anion. McGeoch (Ref. 30) has suggested that a Li^- source should be possible through a series of reactions similar to those found for H_2. The initial step involves the formation of the Li_2 dimer and excitation to low-lying excited states via fast electron collisions or photon pumping. The latter process is that currently being investigated by McGeoch. The reactions are:

$$e \text{ (fast)} + Li_2 \, [X \; {}^1\Sigma_g^+] \rightarrow Li_2^* \, [A \; {}^1\Sigma_u^+, B \; {}^1\Pi_u] + e \tag{1}$$

or

$$Li_2 \, [X \; {}^1\Sigma_g^+] + h\nu \rightarrow Li_2^* \, [A \; {}^1\Sigma_u^+, B \; {}^1\Pi_u] \tag{2}$$
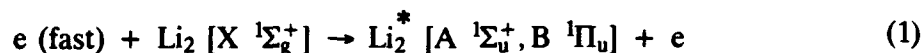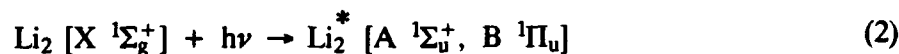
The $A \; {}^1\Sigma_u^+$ and $B \; {}^1\Pi_u$ states both exhibit fast radiative decay back to the ground $X \; {}^1\Sigma_g^+$ state but the Franck–Condon transitions favor a shift in the population of Li_2 to higher vibrational states:

$$Li_2^* [A \; {}^1\Sigma_u^+, B \; {}^1\Pi_u] \rightarrow Li_2^\ddagger \, [X \; {}^1\Sigma_g^+ \, (\nu > 5)] + h\nu \tag{3}$$
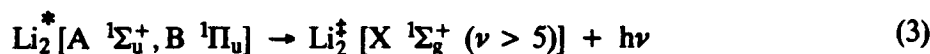
Our present understanding of the energetics of the Li_2/Li_2^- system is shown in Figs. 1 and 2. The dashed curves in Fig. 1 were estimates based on H_2^- and the known molecular orbital structure of Li_2^-. Our most recent *ab initio* calculations, which indicate that the lowest ${}^2\Sigma_g^+$ state of Li_2^-, is slightly attractive all the way into the curve–crossing with the ground state of Li_2, are shown in Fig. 2. This suggests that electron dissociative-attachment is possible for this system for

vibrationally excited Li_2 molecules:

$$e \text{ (slow)} + Li_2^{\ddagger} [X \ ^1\Sigma_g^+] \rightarrow Li \ [^2S] + Li^-[^1S] \tag{4}$$
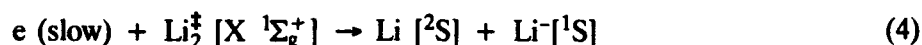
The final potential energy curves governing reaction (4) are shown in Fig. 2. There is still considerable uncertainty in the location of the excited reasonant states of Li_2^-, especially in the auto–ionizing region above Li_2 + e. The ground $[X \ ^2\Sigma_u^+]$ state is well characterized theoretically (Refs. 31, 32) but little is known about the location of the low–lying excited electronic states which connect to $Li \ [^2P] + Li^-[^1S]$. In addition, by analogy with H_2^-, low–lying electronic states of Li_2^- with MO configuration $(1\sigma_g^2 \ 1\sigma_u^2 \ 2\sigma_g 1\pi_u^2)[^{2,4}\Sigma_g^+]$ may, in fact, actually lie lower than some of the states shown in Fig. 1. Such states dissociate to very high atom–ion limits and their general characteristics are uncertain. The curves shown in Fig. 2 represent our best estimates at the present time but more definitive calculations are required to define the curve–crossing regions for dissociative–attachment.

The lowest $^2\Sigma_g^+$ state of Li_2^- has the molecular orbital configuration $[1\sigma_g^2 \ 1\sigma_u^2 \ 2\sigma_u^2 \ 2\sigma_g]$ for large separations. At short internuclear separations, this state mixes with a second bound $^2\Sigma_g^+$ state arising from $Li \ [^2P] + Li^-[^1S]$ with a molecular orbital configuration $[1\sigma_g^2 \ 1\sigma_u^2 \ 2\sigma_g^2 \ 3\sigma_g]$. This mixing at intermediate separations results in a lowering of the interaction potential for the lowest $^2\Sigma_g^+$ state. Our preliminary calculations, as shown in Fig. 1, indicate that this mixing is stronger than expected from MO considerations and lowers the $^2\Sigma_g^+$ potential curve into a feasible region for dissociative–attachment to occur.

The resonance structure associated with electron scattering by the hydrogen molecule has been the subject of many theoretical and experimental studies (Refs. 11, 33, 34). In contrast, electron scattering by Li_2 has received relatively little attention. Miller, et al. (Ref. 35) have measured total cross sections for e + Li_2 scattering in the 0.5–10.0 eV region and find a very large ($\sim 500 \ \text{Å}^2$) and rising total cross section for the low–energy region. These results suggest that some sort of shape resonance may be found in this system corresponding to a low–lying state of Li_2^-. Such resonant states have been observed in electron impact excitation of Na_2 (Ref. 36).

In order to clarify the electronic structure of the Li_2 anion, a series of detailed *ab initio* calculations of the parent $^1\Sigma_g^+$ state of Li_2 and of several possible symmetries of the anion were undertaken. The calculational framework that was chosen was a configuration–interaction (CI) expansion built from orthonormal Slater-type orbitals (STO's). An extended (14σ, 6π, 2δ) basis was optimized using several methods of approach. Complete orbital optimization was possible only for Li_2 and the ground X $^2\Sigma_u^+$ state of Li_2^- since the excited anion states are either autodetaching at some critical internuclear separation or are pure resonant states. The lowest $^2\Sigma_g^+$ state of Li_2^-, which is the principle channel for DA of e + Li_2, is variationally stable for large internuclear separations, and a smooth extrapolation of optimized orbital exponents for this state was carried out into the autodetaching region. The purely resonant states of Li^- and Li_2^- were treated using a modified nuclear charge hamiltonian, similar to that described by Nestmann, et al. (Ref. 37). In this method the resonant states are variationally stabilized by an increased nuclear charge and an analytic extrapolation is carried out to determine the real part of the expectation value of the unperturbed hamiltonian.

Our calculated electron affinity for Li_2, derived from our location of the X $^2\Sigma_u^+$ state of Li_2^-, is 0.42 eV, in good agreement with previous theoretical studies. The A $^2\Sigma_g^+$ state of Li_2^- exhibits a complex potential energy for internuclear separations smaller than 3.45 Å, where a crossing with X $^1\Sigma_g^+$ state of Li_2 is found. This resonant state of Li_2^- is mainly of the Feshbach type and has a long lifetime against autoionization. We find a small width for decay to the ground state of Li_2, $\Gamma(R) \simeq 0.01$ k(R). Of special interest is the low–lying $^2\Pi_u$ resonant state which lies approximately 150 meV above the ground state of Li_2. This anion state has a dominant MO configuration of $(1\sigma_g^2 1\sigma_u^2 2\sigma_g^2 1\pi_u)$, indicating a relatively large capture width for low–energy electron scattering, and is probably responsible for the large scattering cross sections observed by Miller, et al. (Ref. 35) for low collisional energies. The character of this $^2\Pi_u$ state is similar to the $^2\Pi_g$ resonant state of N_2^- in that the anion state lies lower than the corresponding neutral parent for a wide region of internuclear separations ($3.5 \leq R \leq 9.0$ Å).

Further theoretical studies of these interaction potentials are required to define the overall reactive kinetics leading to Li^- production. A study parallel to that reported by Hiskes (Ref. 38) for H_2 has been carried out to estimate the overall cross sections for production of vibrationally excited Li_2. In this study, cross-sections for vibrational excitation (VE) of the X $^1\Sigma_g^+$ state of

Li_2 via formation of the excited A $^1\Sigma_u^+$ or B $^1\Pi_u$ electronic states were reported. For vibrational excitation through the A $^1\Sigma_u^+$ state, the cross sections are nearly constant for forming $3 \leq v'' \leq 9$ via electron collisional excitation. For photon pumping (670 nm $\leq \lambda \leq$ 700 nm) of the A $^1\Sigma_u^+$ state, levels $v'' \leq 9$ are predominantly formed. Vibrational excitation via the B $^1\Pi_u$ state has a lower probability. In addition, theoretical studies are in progress to estimate the low-energy electron dissociative attachment cross-section for $e + Li_2^{\ddagger} \rightarrow Li + Li^-$. Our initial results are shown in Fig. 3 which indicate an attachment cross section $> 10^{-16}$ cm^2 for vibrationally excited Li_2. The enhancement in the attachment cross section with vibrational energy is similar to that found for the $e + H_2^{\ddagger}$ attachment.

In addition to our studies of the Li_2/Li_2^- system, additional calculations were carried out on the He_2^- metastable anion. The existence of metastable negative ions has been the subject of several recent experimental and theoretical investigations (Refs. 19-21). Although much attention has been given to the problem of atomic anion formation, more recent studies have examined diatomic anions, especially those of the lighter elements (Refs. 22-25). In a recent study (Ref. 23), we have examined the electronic structure of the newly discovered (Ref. 22) metastable He_2^- ion using CI wavefunctions. This study indicated that only the $^4\Pi_g$ state of the He_2^- was metastable relative to He_2 $[a^3\Sigma_u^+]$ + e, with an indicated electron affinity of 0.233 eV and a vibrational frequency (ω_e) of 1783.0 cm^{-1}. A low-lying $^4\Sigma_g^+$ resonance state of He_2^- was also found but it was not possible, within the error of the calculations, to ascertain whether or not this state might also be metastable.

More recently, by double charge exchange of He_2^+ ions in lithium vapor, Kvale, et al. (Ref. 26) have examined the autodetachment spectrum for $^4He_2^-$ and $^3He_2^-$ ions and have observed two autodetachment peaks. The first (low-energy) peak was identified as autodetachment from the first vibrational level of He_2^- $[^4\Pi_g]$ to He_2 $[a^3\Sigma_u^+]$ + e and the second as autodetachment to the He_2 $[^1\Sigma_g^+]$ + e repulsive continuum, similar to that observed by Bae, et al. (Ref. 22). This experiment by Kvale, et al. suggested that either the low-energy autodetachment was from the first excited vibrational level of the $^4\Pi_g$ state as postulated, or from a second metastable electronic state (possibly $^4\Sigma_g^+$) lying in this same energy range. In either case, our earlier results, which indicated that the first excited vibrational level of the $^4\Pi_g$ state was non-autodetaching and that

9

the lowest $^4\Sigma_g^+$ state was purely resonant in character, were in disagreement with these experimental observations.

In order to clarify the spectroscopy of He_2^-, a re-examination of both the a $^3\Sigma_u^+$ state of He_2 and the low-lying symmetries of He_2^- was carried out. Our previous studies of this system were based on CI wavefunctions constructed from a $(14\sigma, 6\pi, 2\delta)$ STO-MO basis. The atomic orbital parameters were taken from optimized calculations for the $^4P^\circ$ state of He^-. In these new calculations, a complete non-linear orbital optimization was carried out at the equilibrium internuclear separations. This non-linear optimization was performed separately for both the neutral and negative ion states in an attempt to quantitatively characterize the small energy shifts arising from polarization effects in the formation of the anion. This approach permitted examination of smaller changes in the charge distribution, upon anion formation, than would have been possible by fixed basis set expansions with exponents chosen to insure freedom from linear dependency problems.

For studies of the lowest $^4\Sigma_g^+$ state, a modified nuclear charge hamiltonian was employed similar to the method described by Nestmann and Peyerimhoff (Ref. 39). Stabilization of this state (relative to He_2 $[a^3\Sigma_u^+]$ + e) was realized by increasing the nuclear charge by $\sim 0.1\%$. A careful study of the non-linear parameters as a function of increased nuclear charge clearly indicated that the lowest $^4\Sigma_g^+$ state is purely resonant in character and that this state is autoionizing relative to He_2 $[a^3\Sigma_u^+]$ + e . We find that this lowest $^4\Sigma_g^+$ state lies 0.074 eV above He_2 $[a^3\Sigma_u^+]$ and has a dominant MO structure of $(1s\sigma_g^2\ 1s\sigma_u\ 2s\sigma_g\ 2s\sigma_u)$. A preliminary analysis of the complex part of the potential indicates that this state has a large width for decay to the He_2 $[a^3\Sigma_u^+]$ + e continuum and is unlikely to be observable on the time scale of the detection apparatus in the double charge exchange experiments. Further calculations on the $^4\Sigma_g^+$ and other low lying resonances in He_2^- are required to define the real and complex behavior of these states.

The lowest $^4\Pi_g$ state of He_2^- was found to be variationally stable for all internuclear separations that were examined. Our final potential curve for this state is displayed in Fig. 4. We find an electron affinity of 0.182 eV for the $^4\Pi_g$ state of He_2^-, a value ~ 50 meV smaller than in our previous calculations which employed an STO basis that was optimized for the $^4P^\circ$ (1s2s2p) state of He^-. We attribute this smaller calculated electron affinity to our observation that the use of optimized basis functions resulted in a larger improvement in the calculated energy of

He_2 [$a^3\Sigma_u^+$] than to the corresponding He_2^- [$^4\Pi_g$] anion. Our predicted electron affinity, coupled with a calculated vibrational spacing of 1702 cm^{-1}, now indicates that the first excited vibrational level of the $^4\Pi_g$ state of He_2^- is autoionizing and is probably responsible for the observed low energy peak in the electron detachment studies of Kvale, et al. (Ref. 26). Their experimental estimate (0.175 eV) of the electron affinity of the $^4\Pi_g$ state of He_2^-, relative to He_2 [$a^3\Sigma_u^+$], and our calculated value (0.182 eV) are within the uncertainties of both the experimental measurements and calculations.

In a related study at SRI, Bae, Coggiola and Peterson (Ref. 22) have measured the energy spectrum resulting from electron autodetachment from the lowest $^4\Pi_g$ state of He_2^-. This continuum spectrum exhibits a single peak at 15.7 eV resulting from a vertical transition from He_2^- to the repulsive ground state of He_2. Both the shape and position of this autodetachment spectrum were verified in later studies reported by Kvale, et al. (Ref. 26). However, neither the shape or position of the experimental spectrum seemed to fit predictions based on our He_2^- calculations and the generally accepted ground state He_2 potential reported by Foreman, et al. (Ref. 40).

In order to resolve this discrepancy, Michels and Peterson (Ref. 41) jointly analyzed the He_2 continuum spectra reported by Huffman et al. (Ref. 42) and concluded that the Foreman ground state potential for He_2 was essentially correct. An exhaustive study by Michels and Peterson (Ref. 43) of possible shapes of the potential energy curves for He_2^- resulted in the conclusion that the He_2^- beam must have been rotationally hot in the SRI experiments. A suitable fit to the experimental spectrum was obtained by assuming a rotational temperature of $\sim$ 15000 K, with significant contributions from higher vibrational levels of He_2^-. This collaborative experimental and theoretical effort solved a formidable problem but introduced new questions concerning our understanding of electron autodetachment processes. Our conclusions that vibrational autodetachment must be slow in the He_2^- system runs counter to previous ideas and suggests that electron coupling mechanisms must be reexamined.

2. Hydrogen Cation and Anion Cluster Formation Studies

There have been numerous thermochemical and kinetics studies of weakly bound ionic clusters during the past decade (Refs. 44 and 45). Of particular interest are the H_n^+ cation and H_n^- anion sequences since they represent examples of the chemistry of strong chemical bonding, in H_3^+, the simplest hydrogen bonded molecular ion, in H_5^+, and the simplest atomic anion,

H^-. In addition, for the first few members of these sequences, detailed *ab initio* quantum mechanical calculations of their equilibrium bond lengths and vibrational spectra can be carried out.

Very recently, the possibility of forming large H_n^+ clusters ($n > 1000$), that could be kept for long periods of time in a Penning trap, has been discussed (Ref. 46). Such a system is a prototype for bulk antiproton or antihydrogen storage, with uses as high energy density material or as an energy source for advanced propulsion concepts. The mechanism for formation and storage of these large cluster ions can be understood only if the thermodynamics and kinetics of the cluster growth processes are identified and analyzed in detail. The purpose of our study was to examine the thermodynamic stability of the first few members of the hydrogen cation and anion cluster sequences since their stability is a requirement for defining a useful association pathway for the growth of large clusters.

Numerous experiments (Refs. 47 and 48) have measured the stability of the odd-membered hydrogen clusters that are formed by the association reaction:

$$H_n^+ + H_2 \rightarrow H_{n+2}^+ \; ; \; n = 3, 5, 7, \ldots \tag{5}$$
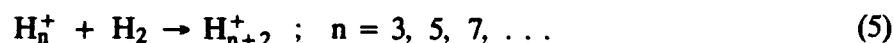
These clusters exhibit stabilization energies of approximately 3–6 kcal/mol, in good agreement with theoretical calculations (Refs. 49 and 50). Until recently, the even-membered hydrogen clusters have not been observed, with the exception of the suggestion of a stable H_4^+ ion formed by the attachment of a H atom to the H_3^+ ion (Ref. 51). A very recent study of the even-membered clusters (Ref. 52) suggests that the H_4^+ observation could be interpreted as H_2D^+. This study also indicates a high degree of stability for H_6^+.

In contrast, the negative hydrogen ion clusters have never been observed and a recent careful search for stable or metastable H_2^- and H_3^- produced negative results (Ref. 53). There have been several theoretical studies (Refs. 54 and 55) which support the existence of stable H_3^-, and higher clusters, but more accurate *ab initio* calculations (Ref. 56) shed doubt on this conclusion.

In order to establish the thermodynamic stability of these hydrogen cluster ions, *ab initio* calculations were carried out to determine their electronic structure and stable geometries. Several Gaussian basis sets, with increasing flexibility, were employed in these studies and levels of theory up to single and double configuration interaction expansions (CISD) were examined.

The results of these calculations are summarized in Table 1, which includes the H^- and H_2 constituents as well as H_3^-. It is clear from Table 1 that the inclusion of the vibrational zero point energy is necessary to assess the stability of H_3^-. We find with every basis and level of theory that the H_3^- ion is not stable with respect to H^- and H_2. This conclusion is supported by the results of earlier theoretical work (Refs. 55 and 56), and by the recent experimental study of Bae, Coggiola, and Peterson (Ref. 53).

Our calculations appear to rule out the formation of hydrogen anion clusters through either of the association reactions:

$$H_n^- + H \rightarrow H_{n+1}^- \tag{6}$$

$$H_n^- + H_2 \rightarrow H_{n+2}^- \tag{7}$$
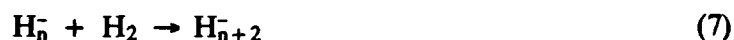
Although previous studies by Hirao and Yamabe (Ref. 56) indicate a weak stability for H_n^- clusters, up to $n = 13$, the non-existence of H_2^- and H_3^- precludes formation of higher clusters through either reaction (6) or (7). There remains the possibility (albeit remote) that association of H^- with a stable Rydberg state of H_3 could produce H_4^-.

3. Resonant Electron Structure of Molecular Anions

Electronic structure calculations of resonant or autoionizing states are usually carried out by stabilization methods or by the use of modified hamiltonians which introduce complex coordinates. The latter methods have the advantage that, for molecular systems, both the real and complex parts of the potential energy surface can be directly defined. The disadvantages include difficulty of application and for some systems, such as Li^- and N_2^-, an ambiguity in the results of several approaches. In a recent paper (Ref. 39), Nestmann and Peyerimhoff have developed a modified hamiltonian method that can be applied to low-lying resonances, basically within a standard CI computational framework. In this method, stabilization of a negative ion state is achieved through a modification of the nuclear charge, $\bar{z} = z(1 + \lambda)$. For a critical value of $\lambda = \lambda_c$, a particular resonance can be stabilized below the autoionization threshold. The quantity

$$E(\lambda) = \langle \psi_s | \mathcal{H}(\lambda) | \psi_s \rangle \tag{8}$$

can be shown to be a quadratic function of λ and a series of calculations for $\lambda > \lambda_c$ yields successive approximations to $E(\lambda)$ that can be extrapolated to yield $E_o = E(\lambda = 0)$, which is the real part of the resonance energy. Development of the complex component can be accomplished by a partitioning technique whereby the total space of the system, $\{\psi_i\}$ $i = 1, n$, is decomposed into a P space spanned by the functions which describe the neutral target and a free electron and a Q space that constitutes the compact component of the resonance. The coupling, k_j, between the compact component of the resonance and the scattering states described with the subspace P can be written as:

$$k_{av} = \left[\sum_{j=1}^{n-1} k_j^2/(n-1) \right]^{1/2} = \left[\sum_{j=1}^{n-1} c_j^2 (E_j - E_o)^2/(n-1) \right]^{1/2} \tag{9}$$

An appropriate resonance width can then be obtained from the Fermi golden rule

$$\Gamma(\epsilon) = 8\pi^2 k_{av}^2 [2\Delta E]^{1/2} \tag{10}$$

where ΔE is the difference between the resonance state energy and that of the neutral target.

We have applied this formalism to the low-lying resonances in the $He/He^-/He_2^-$ and $Li/Li_2/Li_2^-$ systems with good success. Additional studies of the He_2^- resonances are needed since this system is a candidate for studying laser induced transitions from a metastable level. Other ions include Be^- where the $(1s^2 2s2p^2) \rightarrow (1s^2 2s^2 2p)$ transition is of interest, metastable levels in the alkaline earths and molecular anions such as $HeNe^-$, HeH^- and high–lying resonances in H_2^-. Several of these systems are currently being studied experimentally by Compton and co–workers at ORNL, and by Peterson and co–workers at SRI, by means of autodetachment experiments.

4.   R–matrix Calculations of Electron–Molecule Electronic Excitation Collisions

Our studies of vibrational excitation of Li_2, via electron or photon pumping of the electronically excited states, A $^1\Sigma_u^+$ and B $^1\Pi_u$, resulted in relative cross sections, since the electronic excitation cross sections are unknown for this system. Although excitation of the electronic states of a molecule by electron impact is one of the simplest basic processes in molecular collision

phenomena, progress in the theory of this problem has been slow. For a few diatomic molecules, systematic studies (Refs. 57–64) of the excitation cross sections have been made by means of the Born or modified Born approximations. Other approaches have been the R–matrix methods (Refs. 65 and 66), distorted–wave approximation (Ref. 67), the T–matrix method (Ref. 68), and the close–coupling methods as applied to e + H_2 collisions by Chung and Lin (Ref. 69).

For electronic excitation of a molecule through collisions with electrons, the R–matrix method and/or close–coupling techniques would appear to be the most fruitful approaches for low–energy collisions (E ≤ 5 eV). The goal of this research task is to carry out e + H_2 and e + Li_2 calculations to effective convergence with respect to both the orbital basis set and the representation of the target molecule and scattering wave functions. A primary goal is the calculation of electronic excitation cross–sections to the low lying $^1\Sigma_u^+$ and $^1\Pi_u$ states. Converged, fixed–nuclei, electron scattering results of this kind are required for subsequent calculations of nonadiabatic effects in vibrational excitation and dissociative attachment.

Computer programs designed for efficient quantitative calculations of electron–molecule scattering cross sections have been constructed by scientific collaborations involving several research groups. The Belfast/Daresbury group (Refs. 66, 70) has modified the ALCHEMY system of bound state electronic wavefunction programs for molecular R–matrix calculations. Results obtained with Slater orbitals and an artificial center within the molecule (Ref. 71) indicate that this approach is feasible only for low impact energies, because of slow convergence. Oscillatory continuum basis orbital functions are needed to improve convergence. In calculations of e + N_2 scattering, (Ref. 72) numerical solutions of a spherical model potential scattering problem were used as basis orbitals, with satisfactory results up to intermediate energies.

In collaboration with R. K. Nesbet of IBM, we have begun an extension and modification of the present R–matrix code to the CRAY class of computers. In this project, the original IBM-based code will be converted to the CRAY and eventually expanded to include electron–polyatomic molecule scattering within the GAUSSIAN 86 framework.

The present program uses two forms of continuum basis orbitals. Numerical asymptotic functions (NAFs) are generated by solving the coupled multichannel potential problem defined by the static and transition multipole moments of a chosen set of target molecular states and pseudostates. Variational R–matrix calculations include two independent NAFs for each open scattering channel, as energy–dependent basis functions. Effective completeness within the R–matrix boundary r_1 is achieved by including spherical Bessel functions that vanish at r_1, which by themselves define a complete set for each orbital ℓ–value. NAFs are integrated inwards to some inner point, r_0, inside the target charge distribution, where they are matched to regular

spherical Bessel functions. With two NAFs per open channel, the exact multichannel solution of the asymptotic scattering problem is brought inside the R–matrix boundary. Hence the energy–independent continuum basis functions (Bessel functions) are needed only to represent short–range and nonlocal effects.

Programs are under development to compute static and transition multipole moments and the corresponding multipole pseudostates. Pseudostate orbitals are used to describe the dynamical polarization response of the target molecular states. New techniques due to Gailitis (Ref. 73) are used to integrate the asymptotic equations.

Applications of this new code to inelastic e + H_2 scattering was carried out first to check the convergence rate for the wavefunction expansi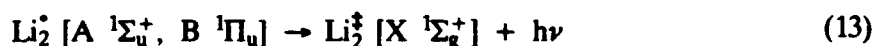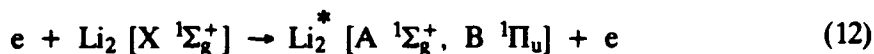on. Comparisons with the theoretical work of Baluja et al. (Ref. 74) and Collins and Schneider (Ref. 75) was made along with analysis of the experimental excitation cross section data. Attention will then be focused on the e + Li_2 system. In particular, cross sections was calculated for vibrational and electronic excitation. For low energy electrons, direct vibrational excitation probably occurs through formation of a resonant Li_2^- structure:

$$e + Li (v'') \rightarrow Li_2^- \rightarrow e\ Li_2^{\ddagger} (v > v'') \tag{11}$$
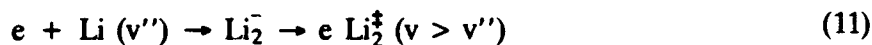
High energy electrons excite the vibrational levels of Li_2 via the indirect mechanism that we have previously described (Ref. 76):

$$e + Li_2\ [X\ ^1\Sigma_g^+] \rightarrow Li_2^*\ [A\ ^1\Sigma_g^+,\ B\ ^1\Pi_u] + e \tag{12}$$

$$Li_2^*\ [A\ ^1\Sigma_u^+,\ B\ ^1\Pi_u] \rightarrow Li_2^{\ddagger}\ [X\ ^1\Sigma_g^+] + h\nu \tag{13}$$

For a completely *ab initio* analysis of the dissociative attachment reactions,

$$e + Li_2^{\ddagger}\ [X\ ^1\Sigma_g^+] \rightarrow Li\ [^2S] + Li^-\ [^1S] \tag{14}$$
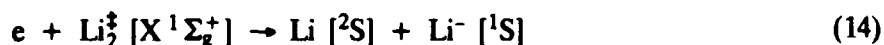
the excitation cross–sections corresponding to Eqs. (11), (12) and (13) must be calculated. Further applications include the e + He_2^* [$a^3\Sigma_u^+$] system and, if computationally practical, the low–lying resonance structure of e + H_2O collisions. This research on dissociative attachment reactions is being carried out in collaboration with Prof. J. M. Wadehra of Wayne State University.

5. Laser Induced Transitions in Negative Ions

In the presence of a strong laser field, the collision of an electron with a neutral atom (or molecule) that has a thermodynamically stable anion may result in resonant attachments. This process was first suggested by R. Compton (Ref. 77) and has been analyzed in some detail by Mittleman (Ref. 78). Using Li^- as a prototype system the overall process would be:

$$e + Li\ [^2S(2s)] \rightarrow Li^-\ [^1P(2s2p)] \tag{15}$$
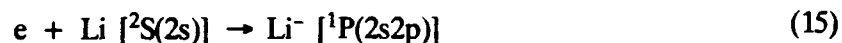
$$laser \left[\frac{\vec{E}(t)\sin \nu t}{\nu} \cdot \vec{P}_N \right] + Li^-[^1P(2s2p)] \rightarrow Li^-[^1S(2s^2)] + h\nu \tag{16}$$

For monoenergetic electrons, with $E_e = E(Li^-\ ^1P) - E(Li\ ^2S)$, stimulated emission from the resonant ^1P state of Li^- should occur for a laser frequency such that

$$h\nu = E(Li^-\ ^1P) - E(Li^-\ ^1S) = E_e + E_a . \tag{17}$$

The detailed analysis of laser induced radiative attachment (and resonance excitation) requires a field dependent hamiltonian such that relaxation effects of the neutral atom are treated in a self–consistent fashion. One approach that might prove fruitful is a modification of a variational scattering formalism to include induced field effects.

We have implemented an expansion technique for inelastic electron–atom scattering (Ref. 79) that might be applied to the field–dependent case provided certain bound–free integrals can be evaluated. Our experience in this area dates back some twenty years and the integral problem can probably be solved in a satisfactory manner.

Our expansion technique formalism follows closely along the developments of Kohn and Hulthén. For the central–field (laser off) Hamiltonian $\mathcal{H}$ of finite range (as would be encountered

in electron–neutral particle scattering) and at a given energy E, we consider approximate stationary-state wavefunctions ψ, of the general form.

$$\psi = \sum_{i=1}^{2n} a_i \, \phi_i + \sum_{i=1}^{n} b_i \, \eta_i \qquad (18)$$

Here the ϕ_i are the complete set of asymptotic eigenfunctions (unbound states) appropriate to energy E, and the η_i are quadratically integrable short–range functions needed to approximate ψ within the range of $\mathcal{H}$. In most implementations of the R–matrix method, only the set of η_i are included but with the addition of conditioned functions capable of an approximate description of the asymptotic region.

In a n–channel problem there will be n different stationary–state wavefunctions to be approximated by Eq. (18). All scattering processes can be characterized from the a_i coefficients of these wavefunctions since the a_i define the relative amplitudes and phases in the various channels. To variationally determine these wavefunctions, we assume the expansion

$$(\mathcal{H} - E) \, \psi = \sum_{i=1}^{2n} c_i \, \phi_i + \sum_{i=1}^{n} d_i \, \eta_i \qquad (19)$$

Equation (19) amounts to the assumption that short–range functions beyond those important in ψ do not contribute appreciably to $(\mathcal{H} - E) \, \psi$. Combining Eqs. (18) and (19) and taking scalar products with η_i and ϕ_i, we have

$$M_{\eta\phi} \, \underline{a} + M_{\eta\eta} \, \underline{b} = \underline{d} \qquad (20)$$

$$M_{\phi\phi} \, \underline{a} + M_{\phi\eta} \, \underline{b} = N c \qquad (21)$$

where the $M_{\eta\phi}$, + $M_{\eta\eta}$, etc., are matrices of $< \eta_i | \mathcal{H} - E | \phi_j >$, $< \eta_i | \mathcal{H} - E | \eta_j >$, etc. The solution of Eqs. (20) and (21) can be accomplished in several approximations (Refs. 79 and 80).

Introduction of the laser field as a perturbation to the $n + 1$ electron hamiltonian $\mathcal{H}$ now requires that

$$\left[i \frac{\partial}{\partial t} - \mathcal{H}'(h\nu) \right] \psi'(t) = 0 \qquad (22)$$

with $\mathcal{H}' = \mathcal{H} - E(t) \dfrac{\sin \nu t}{\nu} \cdot \vec{p}_N$ and subject to the constraint that the central–field hamiltonian satisfy a self–consistent minimization condition

$$(\mathcal{H} - E_c) \, \psi = \text{minimum} \qquad (23)$$

The function, $\psi = \{\psi_i\}$ $i = 1, \ldots n$, can be decomposed into a P space spanned by functions which describe the distorted neutral target plus the electron and a Q space that describes the compact resonant state. Then, to first order, the transition from the resonant part of $\mathcal{H}\psi_{res} = Q \, \mathcal{H} \, Q$, to the final negative ion state ψ_f^- is governed by the matrix element

$$< \psi_f^- | \vec{e} \cdot \vec{p}_N \, | \psi_{res} > \qquad (24)$$

where ψ_f^- is variationally constructed from the functions $\{\psi_i\}$ $i = 1, \ldots n$ and projected to be orthogonal to the resonant state.

Although modified field hamiltonians, within a self–consistent formulation, have been used in calculations of dipole polarizabilities, the time dependance introduced through Eq. (22) must now be treated by successive approximations. The matrix element calculations remain a formidable task.

6. Ion–Pair Formation in Rydberg Atom Collisions

The negative ions of light atoms are currently being studied for their possible application in gaseous discharges, fusion plasmas and gas lasers (Ref. 81). Our source for the volume production of atomic anions is the process of dissociative electron attachment to molecules (Ref. 82). This process has been studied experimentally for low energy electron–hydrogen molecule collisions by

Allen and Wong (Ref. 83). A parallel theoretical study has been reported by Wadehra and Bardsley (Ref. 84). More recently, McGeoch and Schlier (Ref. 85) have examined dissociative attachment (DA) in electron–lithium molecule collisions and have found large DA rates for attachment to highly vibrationally excited Li_2 molecules. The effect of vibrational excitation on the DA rates has been studied by Hiskes (Ref. 86) for e + H_2 collisions and by Wadehra and Michels (Ref. 87) for the e + Li_2 system.

In the e + Li_2 system, it has been shown (Ref. 87) that excitation of Li_2 to the A $^1\Sigma_u^+$ state, either by electron impact or by photon pumping, results in an enhanced vibrational distribution upon radiative decay of the A $^1\Sigma_u^+$ state to the ground X $^1\Sigma_g^+$ state of Li_2. The cross sections for vibrational excitation of Li_2 X $^1\Sigma_g^+$ via low energy electron collisional excitation of the A $^1\Sigma_u^+$ state exhibit a relatively flat vibrational distribution in the range $3 \le v'' \le 9$. This suggests that Li_2 molecules which are vibrationally excited to the DA threshold for Li^- formation should exhibit the largest attachment cross sections, a result that is indicated by the studies of McGeoch and Schlier (Ref. 85).

An alternative mechanism for negative ion formation was suggested by Lee and Mahan (Ref. 88), who proposed that ion–pair formation:

$$X^* + X \rightarrow X^+ + X^- \tag{25}$$

should occur for systems where the energetics for ion–pair formation are competitive with associative ionization:

$$X^* + X \rightarrow X_2^+ + e. \tag{26}$$

The alkali metals, including lithium, are therefore good candidates for such a study of ion–pair formation. Ciocca, et al. (Ref. 27) have recently reported on the formation of Na^- ions in highly excited (n = 7–40) Rydberg atom collisions. In a similar experiment, Cheret and Barbier (Ref. 28) have reported efficient ion–pair formation in collisions between ground state and Rydberg Rb atoms formed by laser excitation. A curve crossing mechanism was suggested to explain these results.

More recently, McGeoch and Schlier (Ref. 29) have looked for ion–pair formation in collisions between two Rydberg Li atoms (n = 5-9). The most prominent processed observed was associative ionization:

$$Li^{**} + Li^{**} \rightarrow Li_2^+ + e \tag{27}$$

rather than ion–pair production, which was not observable at a rate ~ 300 times less than associative ionization. McGeoch and Schlier followed the time dependence for the formation of Li^- and find that it follows the production route by associative ionization of $e + Li_2$. These results, for the first time, rule out direct ion–pair formation as an important process, at least in Li atom collisions, and suggest that the earlier work of Ciocca, et al. (Ref. 27) and Cheret and Barbier (Ref. 28) may be subject to a different interpretation.

In order to determine the possible paths for alkali excited state interactions, we have undertaken a series of *ab initio* calculations of the electronic states of Li_2 up to the $Li [^2S(3s)] + Li [^2S(3s)]$ dissociation limit. Since the formation of the ion–pair $Li^+ [^1S] + Li^- [^1S]$ can occur only for $^1\Sigma_g^+$ and $^1\Sigma_u^+$ symmetries, we have restricted our studies to these two representations (see Table 2).

Theoretical potential curves for the $^1\Sigma_g^+$ and $^1\Sigma_u^+$ symmetries of Li_2 were obtained from valence configuration interaction (VCI) calculations. A 64 function Slater orbital basis, containing a (2s1p) optimized valence basis augmented by a (3s3p3d2f) Rydberg basis, was used in this study. The basis was transformed to $D_{\infty h}$ symmetry orbitals and CI calculations were performed in the space of all symmetry adapted configurations having the $1\sigma_g$ orbital doubly occupied. The resulting CI expansions contained 344 and 331 configurations for the $^1\Sigma_g$ and $^1\Sigma_u$ symmetries, respectively. As the interactions in this system are very long–range, calculations were performed over a range of internuclear separations from 5 to 50 bohrs.

The results of our theoretical calculations are shown in Fig. 5 and Fig. 6 for the $^1\Sigma_g^+$ and $^1\Sigma_u^+$ symmetries, respectively. The ionic curves which dissociate to $Li^+ [^1S] + Li^- [^1S(2s^2)]$ are clearly evident in both Fig. 5 and Fig. 6, where they exhibit a nearly diabatic crossing behavior

with the normal valence states of Li_2 at large internuclear separations, but show strong mixing at distances $\leq 10\,\text{Å}$. Ion–pair formation may occur for long-range interactions of the type

$$Li\ [^2S(2s)]\ +\ Li^{**}\ [^2S(n\ =\ 5)]\ \rightarrow\ Li^+\ [^1S]\ +\ Li^-[^1S] \tag{28}$$

but clearly there are few effective curve crossing channels leading to $Li^+\ +\ Li^-$. The curve crossing mechanism suggested by Ciocca, et al. (Ref. 27), thus appears not to be an important mechanism for ion–pair production in the Li_2 system.

A second mechanism suggested by Ciocca et al. (Ref. 27) for alkali negative ion formation would involve excited state negative ion formation via

$$Li^*\ [^2P(2p)]\ +\ Li^{**}\ (n\ \geq\ 9)\ \rightarrow\ Li^+\ [^1S]\ +\ Li^-[^1P(2s2p)] \tag{29}$$
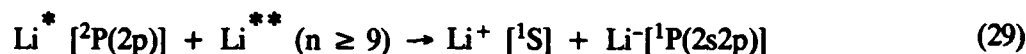
or from electron attachment to a Rydberg state of Li^{**} followed by radiative stabilization to the ground $Li^-\ [^1S(2s^2)]$ state. Both of these processes can be ruled out for the Li_2 system since the autoionization lifetime of the $Li^-\ [^1P(2s2p)]$ state is known to be very short (Ref. 89) relative to radiative stabilization and higher autoionizing states should exhibit even shorter lifetimes.

As mentioned above, McGeoch and Schlier (Ref. 29) have recently found that the most prominent process occurring in lithium Rydberg atom collisions is associative ionization:

$$Li^{**}\ +\ Li^{**}\ \rightarrow\ Li_2^+\ +\ e \tag{30}$$

This reaction has excess exothermicity beyond the dissociation energy of Li_2^+. Some mechanism for disposing this excess energy must be developed, either by radiation or by internal modes. It is very unlikely that the excess energy is released as kinetic energy since very hot electrons would be formed which would result in secondary ionization processes. An alternate possibility is that an excited metastable state of Li_2^+ is formed with sufficient lifetime to be detected and mass analyzed.

Finally, a careful experimental crossed beam study of He Rydberg atom–alkali Rydberg atom interactions has been suggested by J. Peterson (SRI). This study would include kinetic

energy analysis of the products as well as laser selected reactants. The main reaction appears to form a direct ion–pair production mechanism:

$$He^{**} \, [^3S(2s)] \; + \; K^*_{Rydberg} \, (Rb) \; \rightarrow \; He^- \; + \; K^+(Rb^+) \tag{31}$$

The interaction potentials and energetics of such excited state noble gas–alkali collisions are unknown.

7. Dissociative Attachment Studies

The process of dissociative electron attachment to a molecule is understood (Ref. 90) to proceed via the intermediate formation of an electron–molecule resonance that is capable of autodetaching the temporarily bound electron with a finite lifetime that is related to the width, Γ, of the resonance. The potential curves of the neutral molecule (H_2, Li_2 or LiH) and of the resonant state (He_2^-, Li_2^-, $Li\,H^-$) cross at an internuclear separation $R = R_s$ such that, for $R \geq R_s$, the autodetachment of the electron is energetically not possible and the resonance turns into a stable bound state. The cross section for dissociative electron attachment is determined by the asymptotic value of the radial nuclear wave function $\xi(R)$ of the resonant state. Using energy normalized continuum functions, we have:

$$\sigma_{DA} \; = \; \frac{\pi}{k_i^2} \left\{ \frac{2\pi\hbar^2 K}{M} \lim_{R \to \infty} |\xi(R)|^2 \right\} \tag{32}$$

Here $\hbar K/M$ is the relative velocity of the ion–atom pair after the attachment process. Note that the geometrical cross section, π/k_i^2, provides an upper bound (Ref. 91) to the attachment cross section since the quantity within the curly parenthesis can be interpreted as a product of two probabilities, one for the capture of an electron to form the resonant state and the other (often called the survival probability) for the nuclei in the resonant state to separate out to the stabilization radius R_s. Using a semiclassical analysis the cross section for dissociative electron attachment, σ_{DA}, can also be written as (Ref. 92) a product of two factors:

$$\sigma_{DA} \; = \; \sigma_{cap} S \tag{33}$$

The first factor, σ_{cap}, is interpreted as the cross section for the formation of a resonant anion state by the capture of the incident electron and the second factor S (the survival probabili-

ty) is interpreted as the probability that the separation of the nuclei in the resonant anion state increases up to the stabilization radius R_s without electron autodetachment having occurred. This separation ensures that the process of dissociative electron attachment will occur. The survival probability S, in the semiclassical analysis, is approximated by

$$\exp(-\bar{\Gamma}\tau/\hbar) \tag{34}$$

where τ, the time taken by the nuclei to separate after resonance formation to the stabilization R_s, is directly proportional, by simple kinematical considerations, to $M^{1/2}$. $\bar{\Gamma}$ is the average width of the resonance.

The computational aspects of Eq. (32) consist of: a) accurate potential energy curves for the neutral and corresponding negative ion species over a range of internuclear separations (R) from the repulsive wall to separated atom states and b) calculation of the R dependence of the complex part of the potential, $\Gamma(R)$. The latter calculation is relatively difficult and usually involves some type of extrapolation from a modified nuclear system charge or a direct analysis in complex coordinates.

The LiH and Li H⁻ systems were studied using the DIATOM (Ref. 93) molecular structure code with a $[13\sigma, 6\pi, 2\delta]$ STO basis. These STO basis calculations were required to examine the relative behavior of the LiH and Li H⁻ species at very short internuclear separations and to insure correct asymptotic behavior. The non-linear STO parameters were optimized to describe the asymptotic negative atomic ions, Li⁻ and H⁻. The variationally determined parameters have been previously reported (Ref. 25). A full CI, with frozen core for Li, was employed to insure correct size consistency at the asymptote limits. The lowest two molecular states of Li H⁻ are variationally stable at large internuclear separations. As the internuclear separation is decreased, the possibility of curve crossing with the neutral ground state of LiH exists and the anion CI framework can become variationally unstable. To treat this problem, we employ a modified nuclear charge Hamiltonian, similar to that described by Nestmann and Peyerimhoff (Ref. 94). The modified Hamiltonian causes the anion states to lower below the corresponding neutral molecule. A systematic extrapolation of the modified Hamiltonian is then employed to predict the location of the molecular anion states in the autodetaching regions.

In order to examine the stability of Li_xH_y clusters, *ab initio* calculations were carried out for several species at the MP2 level of theory. The basis set chosen was the Gaussian 6-311G triple split-valence set (Ref. 95), augmented by d-polarization functions [$\alpha = 0.20$] for Li and p-polarization [$\alpha = 0.75$] for H. In addition, a diffuse s-function [$\alpha = 0.036$] and a diffuse sp-shell [$\alpha = 0.0074$] were added to hydrogen and lithium respectively, to better describe the negative ion

charge distributions. All calculations were performed using CADPAC (Ref. 96), an electronic structure code that can perform geometry optimization and calculate force constant matrices analytically. Optimized geometries were calculated at the MP2 level of theory. Harmonic vibrational frequencies were subsequently calculated at the MP2 stationary points.

The results of our calculations for the LiH and LiH$^-$ systems, using the DIATOM code, are shown in Fig. 7 for states of $^2\Sigma^+$ symmetry of Li H$^-$. In Fig. 8, we illustrate the short range behavior of the lowest and first excited $^2\Sigma^+$ states of Li H$^-$. It is evident that the ground $X^2\Sigma^+$ state of Li H$^-$ is bound, relative to $X^1\Sigma^+$ of LiH, for all internuclear separations. Our calculated adiabatic electron affinity is 0.33 eV, in good agreement with previous theoretical studies (Ref. 97). The first excited $^2\Sigma^+$ state of Li H$^-$, which asymmetrically correlates to Li$^-$ + H, exhibits repulsive behavior in the region $3.0 \leq R \leq 6.0$ Å. Thus, dissociative attachment of e + LiH mainly forms Li$^-$ for $E_{coll} \geq 3.0$ eV. The formation of Li + H$^-$ products may occur by non–adiabatic coupling of the $X^2\Sigma^+$ state of Li H$^-$ to the continuum of e + LiH [$X^1\Sigma^+$] for $E_{coll} \geq 2.1$ eV. However, the cross section for such an indirect electron capture mechanism is predicted to be very small.

Figure 9 shows a comparison of the potential curves of the ground states of the molecules H$_2$, LiH and Li$_2$ as well as the potential curves of the states of the corresponding molecular anions that are primarily responsible for dissociative electron attachment to these molecules. As one progresses from H$_2$ to LiH to Li$_2$, the equilibrium internuclear separation increases from 1.40 a.u. to 3.08 a.u. to 5.06 a.u. and the dissociation energy of the molecule decreases from 4.73 eV to 2.33 eV to 1.06 eV. Furthermore, the energy spacing between the same two low–lying adjacent vibrational levels decreases as one proceeds from H$_2$ to LiH to Li$_2$, in such a manner that the total number of bound vibrational levels increases on increasing the molecular mass. These energetics have different quantitative effects on the threshold for dissociative electron attachment to these molecules as well as on the factor by which the attachment cross section is enhanced on vibrationally exciting these molecules. The threshold energy for dissociative attachment to a molecule that is rovibrationally excited to a particular level (v,J) is $E_{th}^{DA} = D-EA-E_{vJ}$, if E_{vJ} < D–EA, and $E_{th}^{DA} = 0$ otherwise. The lower energy threshold for dissociative attachment thus enhances the attachment cross sections as we proceed from H$_2$ to LiH to Li$_2$.

The possible role of Li$_x$H$_y$ clusters was examined through *ab initio* calculations of Li$_2$H, Li$_3$H, Li$_2$H$_2$ and their respective negative ion states. All clusters calculations were carried out using the CADPAC code. Optimized geometries were calculated at the MP2 level of theory. Harmonic vibrational analyses were subsequently computed at the MP2 stationary points. In several instances, the cluster anion is unbound relative to the corresponding neutral molecule. In such cases, a check on vibrational stability is required to insure that there are no instabilities

toward anion decomposition. Further, the endothermicity of the anion calculation must be studied as a function of the addition of diffuse basis functions. The anions studied here did not exhibit a strong energy dependence on the diffuse functions, suggesting that they may represent Feshbach structures. This feature, however, was not explored in detail and some uncertainty can be assigned to our energetics of the thermodynamically unstable anion clusters. In Fig. 10, we illustrate the stationary geometry of Li_2H and the corresponding negative ion. We find that the C_{2v} structure for Li_2H has vibrational stability and is thermodynamically stable relative to $Li_2 + H_2$. In addition, the corresponding C_{2v} anion is slightly bound (0.06 eV) relative to the neutral species. These results are in qualitative agreement with previous theoretical studies of Li_2H by Cardelino, et al. (Ref. 98), that were carried out at the SCF level of theory.

The Li_3H species was examined both as a C_{3v} (trigonal pyramid) and as a C_{2v} (kite–like) structure. Our previous studies (Ref. 99) of Li_3H indicated that, although both structures exhibited stable vibrational frequencies, only the C_{2v} structure was thermodynamically stable. In Fig. 11, we illustrate the two stable geometries of neutral Li_3H. Of these, the C_{2v} structure represents the global minimum for the system. The $Li_3 H^-$ anion is not stable as a C_{3v} structure and collapses to $Li_3 + H^-$. The C_{2v} structure of $Li_3 H^-$ has the stationary structure shown in Fig. 11, but a vibrational analysis indicates that this is probably a saddle region on the potential energy surface. In addition, this region is thermodynamically endothermic by 0.24 eV, relative to the neutral Li_3H.

Finally, calculations were carried out for the $(LiH)_2$ dimer, as a linear ($C_{\infty v}$), rhomboid (D_{2h}) and y–structure (C_{2v}). The results are shown in Fig. 12 where we show that the linear conformation has one imaginary frequency, and thus represents a saddle point on the surface. The C_{2v} structure is totally unstable and collapses to separate $Li_2 + H_2$ molecules. The only vibrationally stable geometry is the $^1A_1$ state as a D_{2h} structure. The corresponding negative ion $Li_2 H_2^-$ is vibrationally unstable and unbound by over 2.0 eV, relative to $Li_2H_2(D_{2h})$.

A summary of the thermodynamics of these Li_xH_y clusters is given in Table 3. All energies are given relative to Li_2 and H_2 as gas phase species. As previously known, the formation of LiH is endothermic by 0.740 eV. However, higher clusters are all thermodynamically stable: Li_2H (–0.280 eV), Li_3H (–1.034 eV) and Li_2H_2 (–1.263 eV).

The trend of our studies to date indicates that large Li_xH_y (and by analogy, Cs_xH_y) clusters are thermodynamically stable. In particular, the Li_2H_2 species, as a C_{2v} structure, may be an important component of alkali–hydrogen mixtures. This species can dissociatively attach an electron to form $Li_2H + H^-$ for $E_{coll} \geq 2.0$ eV. The Li_3H (C_{2v}) species should also exhibit DA to form $Li_3 + H^-$, but the concentration of this molecule will be lower than that of the more stable Li_2H_2 cluster. The mechanism for DA to these Li_xH_y clusters can be understood by following

their intrinsic reaction coordinate pathways leading to dissociation. In addition, the role of higher order clusters in volume DA processes is uncertain.

8. Studies of Negative Ion Thermochemistry

In recent years, the dissociation energy of a C–H bond of acetylene HCCH→H+CCH has been the subject of a number of studies, both experimental (Refs. 100–102) and theoretical (Ref. 103). All of these studies were in close agreement, reporting values or upper bounds for D_0(H–CCH) ranging from 131.9 kcal/mol (Ref. 100) to 133.5 kcal/mol (Ref. 103). However, two very convincing new measurements (Refs. 104 and 105) of this dissociation energy $D_0 \leqslant 126.647 \pm 0.002$ kcal/mol (Ref. 104) and D_0 127 $\pm$ 1.5 kcal/mol (Ref. 105) are in close agreement with Benson's thermochemical estimate (D_0 126 $\pm$ 1 kcal/mol (Ref. 106)) and have raised doubts about the accuracy of the higher values. In an attempt to determine which value is correct, we have performed a new *ab initio* calculation of this dissociation energy including extrapolation to the complete basis set (CBS) limit (Refs. 107–115). Our analysis indicates that the probable error in the new calculation is less than 1 kcal/mol. Our calculated dissociation energy (D_0 131.54 kcal/mol) is consistent with the higher values, but not with the most recent experiments (Refs. 104 and 105).

In conjunction with this analysis of the thermochemistry of C_2H_2, we have calculated the electron affinity of the C_2H radical. The recent accurate measurement of the electron affinity of CCH (2.969 $\pm$ 0.010 eV) by Ervin et al. (Ref. 116) offers an additional opportunity to assess the accuracy of our calculated results. If there is a systematic error in our calculated CCH energy, it would also affect our prediction of the CCH electron affinity. Using the basis set described above, augmented by an additional diffuse carbon d function, we find EA(CCH) = 2.961 $\pm$ 0.015 eV, in excellent agreement with Ervin et al.

Subsequently, Ervin and Lineberger (Ref. 117) reported new experimental values for the electron affinity (2.969 $\pm$ 0.006 eV) and dissociation energy (187.2 $\pm$ 2.5 kcal/mol) of C_2^- (Ref. 117). As a further test of our methodology, we have performed CBS–QCI calculations for comparison with these experimental results. The calculated results are EA (C_2) = 2.92 $\pm$ 0.02 eV, Do (C_2^-) = 188.9 $\pm$ 1.5 kcal/mol and Do (C_2) = 143.7 $\pm$ 1.5 kcal/mol. The calculated values for EA (C_2) and Do (C_2^-) are found to be in good agreement with the experimental results, although the errors slightly exceed our expected values. One interesting point emerges from further comparison. Using a thermodynamic cycle, Ervin and Lineberger derive Do (C_2^-) from their measured value of EA (C_2) and the accurately known value of EA (C), and Do (C_2). For Do (C_2), which their experiment does not determine, they use a value of 141.0 $\pm$ 2.5 kcal/mol, taken from literature values. A higher value of Do (C_2), such as the 143.2 kcal/mol recommended by Herzberg and Huber (Ref. 118) would be in better agreement with our calculated Do (C_2), and in combination with the accurate experimental electron affinities, would give a value (189.4 kcal/mol) for

Do (C_2^-) that is also in better agreement with our theoretical value. Thus, these calculations suggest that the accepted value of Do (C_2) is roughly 2-3 kcal/mol too low.

CBS–QCI studies have also been performed on the vinylidene–acetylene isomerization process, which has been recently observed by Lineberger and co–workers (Ref. 119). The calculated isomerization barrier ($\Delta E_e = 2.2 \pm 0.5$ kcal/mol) and energy change from vinylidene to acetylene ($\Delta E_o = -43.9 \pm 0.5$ kcal/mol) are in excellent agreement with recent experimental values ($\Delta E_e = 2$ kcal/mol, and $\Delta E_o = -43 \pm 2$ kcal/mol). In spite of the small barrier height for this strongly exothermic reaction, the transition state is located halfway between the reactant and product in apparent violation of the Hammond postulate (Ref. 120). We have shown that the potential energy surface for the isomerization can best be understood by considering two distinct processes. The location of the transition state is determined by the hydrogen migration which has a significant barrier, whereas the exothermicity results from the conversion of the lone pair of vinylidene to a π bond in acetylene. Each of these processes individually satisfies the Hammond postulate.

PUBLICATIONS AND PRESENTATIONS

The significant research results obtained under this Contract have been prepared for publication in technical journals or presented at technical meetings. These papers and meetings are listed below. Abstracts of the published papers are included in the Appendices to this report.

A. Technical Reports in Journals and Books

1. *Potential Energy Curves for Dissociative Recombination of HeH$^+$*. H. H. Michels, published as a chapter in Dissociative Recombination: Theory, Experiment and Applications, eds. J. B. A. Mitchell and S. L. Guberman, World Scientific Pub. Co. Inc., 1989, pp. 97–108.

2. *Theoretical Study of Ionization and Electron Attachment Processes in Rydberg Atom Collisions.* H. H. Michels and R. H. Hobbs, SPIE – Microwave and Particle Beam Sources and Directed Energy Concepts, Vol. 1061, 1989, pp. 597–604.

3. *Laser Induced Chemiluminescence of the LiMg Excimer.* G. Pichler, A. M. Lyyra, P. D. Kleiber, W. C. Stwalley, R. Hammer, K. M. Sando and H. H. Michels, Chemical Physics Letters, 156, 1989, pp. 467–471.

4. *Gas Phase Alkali–Hydrogen Interaction in Negative Ion Sources.* H. H. Michels and J. M. Wadehra, Particles and Fields Series 40, Proceedings of the Fifth International Symposium on the Production and Neutralization of Negative Ions and Beams, Conf. Proceedings No. 210, ed. Ady Hershcovitch, p. 142 (Brookhaven, NY, 1989) 1990.

5. *Dissociative Electron Attachment to Light Molecules: A Comparative Study of H$_2$, LiH and Li$_2$.* H. H. Michels and J. M. Wadehra, Particles and Fields Series 40, Proceedings of the Fifth International Symposium on the Production and Neutralization of Negative Ions and Beams, Conf. Proc. No. 210, ed. Ady Hershcovitch, p. 114, (Brookhhaven, NY, 1989) 1990.

6. *On the C–H Bond Dissociation Energy of Acetylene.* J. A. Montgomery and G. A. Petersson, Chemical Physics Letters, 168, pp. 75–78, 1990.

7. *Structure and Stability of Li$_x$H$_y$ Molecules and Anions.* H. H. Michels and J. M. Wadehra, to be published in the International Journal of Quantum Chemistry. Sanibel Symposia Proceedings Supplement, pp. 521–530,1990.

8. Comment on *An Experimental and Theoretical Study of the Negatively Charged Helium Dimer, He$_2^-$.* H. H. Michels, R. H. Hobbs, Y. K. Bae and J. R. Peterson, Chemical Physics Letters, 170, pp. 411–412, 1990.

9. *A Complete Basis Set Model Chemistry. III. The CBS–QCI Family of Methods.* G. A. Petersson, T. G. Tensfeldt and J. A. Montgomery, Jr. submitted to Journal of Chemical Physics, <u>94</u>, pp. 6091–6101, 1991.

10. *Temperature, Kinetic Energy and Rotational Effects in Reactions Involving Isotopes.* A. A. Viggiano, R. A. Morris, J. M. Van Doren, J. F. Paulson, H. H. Michels and R. H. Hobbs, to be published in the American Chemical Society volume on Isotopic Effects in Chemical Reactions and Photodissociation Processes, 1991.

11. *Vinylidene and the Hammond Postulate,* G. A. Peterson, T. G. Tensfeldt and J. A. Montgomery, submitted for publication to the Journal of the American Chemical Society, 1991.

B. Technical Paper and Lecture Presentations

1. *Theoretical Study of Ionization and Electron Attachment Processes in Rydberg Atom Collisions.* Presented at the SPIE's OE/LASE '89 conference, Los Angeles, CA, January 18–20, 1989.

2. *Energetics of Negative Ion Formation via Dissociative Attachment of e + LiH.* Presented at the 1989 Annual Meeting of the Division of Atomic, Molecular and Optical Physics (DAMOP), Windsor, Ontario, Canada, May 17–19, 1989.

3. *Gas Phase Alkali–Hydrogen Interactions in Negative Ion Sources.* Presented at the Fifth International Symposium on the Production and Neutralization of Negative Ions and Beams, held at Brookhaven Lab, NY, October 30 – November 3, 1989.

4. *Dissociative Electron Attachment to Light Molecules: A Comparative Study of H_2, LiH and Li_2.* Presented at the Fifth International Symposium on the Production and Neutralization of Negative Ions and Beams, held at Brookhaven Lab, NY, October 30 – November 3, 1989.

5. *Structure and Stability of Li_mH_n Molecules and Anions.* Presented at the Sanibel Sympsoia, St. Augustine, FL, March 17–24, 1990.

6. *A Theoretical Determination of the C–H Bond Dissociation Energy of Acetylene.* Presented at the National American Chemical Society Meeting, Boston, MA, April 23–27, 1990.

7. *Energies of Neutral and Negative Ions of Li_mH_n Clusters.* Presented at the DAMOP 1990 Annual Meeting, Monterey, CA, May 21–23, 1990.

8.   *Ab Initio Study of the Vinylidene – Acetylene Isomerization Process.* Presented at the
     1991 National American Chemical Society Meeting, New York City, NY, August
     26–29, 1991.

9.   *Energies of the O^- + CH_4 Ion–Molecular Reaction.* Presented at the 1991 Gaseous
     Electronics Conference, Albuquerque, New Mexico, October 20–25, 1991.

REFERENCES

1. Proceedings of the Eighth Symposium of Engineering Problems of Fusion Research. San Francisco, CA, November 1979.

2. Belchenko, Y. I., G. I. Dimov and V. G. Dudnikov: A Powerful Injector of Neutrals with a Surface-Plasma Source of Negative Ions. Nuclear Fusion, 14, p. 113, 1974.

3. Dimov, G. I.: Proceedings of the Second Symposium on Ion Sources and Formation of Ion Beams, Berkeley, CA, 1974.

4. Hiskes, J. R., A. Karo and M. Gardner: Mechanism for Negative-Ion Production in the Surface-Plasma Negative-Hydrogen-Ion Source. Journal of Applied Physics, 47, p. 3888, 1976.

5. Grossman, M. W.: H^- Ion Source Diagnostics. Proceedings of the Symposium on the Production and Neutralization of Negative Hydrogen Ions and Beams. Brookhaven National Laboratory, New York, 1977.

6. Bacal, M. and G. W. Hamilton: H^- and D^- Production in Plasmas. Physics Review Letters, 42, p. 1538, 1979.

7. Nicolopoulou, E., M. Bacal, and H. J. Doucet: Equilibrium Density of H^- in a Low Pressure Hydrogen Plasma. Journal of Physics (France), 38, p. 1399, 1977.

8. Hiby, J. W.: Mass-Spectrographic Investigation of Hydrogen and Helium Canal Rays (H_3^+, H_2^-, HeH^+, HeD^+, He^-). Ann. Physik 34, p. 473, 1939.

9. Holoien, E. and J. Midtdal: On a Metastable Energy State of the Negative Helium Ion, Proceedings of the Physical Society (London), 68, p. 815, 1955.

10. Schulz, G. J.: Resonance in the Elastic Scattering of Electrons in Helium. Physical Review Letters, 10, p. 104, 1963.

11. Schulz, G. J.: Resonances in Electron Impact on Atoms. Reviews of Modern Physics, 45, p. 378, 1973.

12. Edwards, A. K., J. S. Risley, and R. Geballe: Two Autodetaching States of O^-. Physical Review A3, p. 583, 1971.

13. Patterson, T. A., H. Hotop, A. Kasdan and D. W. Norcross: Resonances in Alkali Negative-Ion Photodetachment and Electron Affinities of the Corresponding Neutrals. Physical Review Letters, 32, p. 189, 1974.

14. Mazeau, J., F. Gresteau, R. I. Hall and A. Huetz: Energy and Width of $N^-(^3P)$ From Observation of Its Formation by Dissociative Attachment to N_2 and NO. Journal of Physics B: Atomic and Molecular Physics, 11, p. L557, 1978.

REFERENCES (continued)

15. Spence, D. and P. D. Burrow: Resonant Dissociation of N_2 by Electron Impact. Journal of Physics B: Atomic and Molecular Physics, 12, p. L179, 1979.

16. Walton, D. S., B. Peart and K. Dolder: Structure Observed During Detailed Measurements of Detachment from H^- by Electron Impact. Journal of Physics B, 3, L148, 1970.

17. Hodges, R. V., M. J. Coggiola and J. R. Peterson: Photodetachment Cross Sections for He^- ^4P . Physical Review, A23, p. 59, 1981.

18. Peterson, J. R., M. J. Coggiola and Y. K. Bae: Measurement of the 1s2p2p' $^4P^e$ Resonance in He^- Photodetachment. Physical Review Letters, 50, p. 664, 1983.

19. Alton, G. D., R. N. Compton and D. J. Pegg: Concerning A Long-Lived ($^2P^e$) He^- State: Lifetime and Energy-level Measurements of He^- . Physical Review, A28, p. 1405, 1983.

20. Bunge, C. F., M. Galan, R. Jauregui: Systematic Search of Excited States of Negative Ions Lying Above the Ground State of the Neutral Atom. Nuclear Instruments and Methods of Physical Research, 202, p. 299, 1982.

21. Beck, D. R. and C. A. Nicolaides: Fine and Hyperfine Structure of the Two Lowest Bound States of Be^- and Their First Two Ionization Thresholds. International Journal of Quantum Chemistry Symposium (USA) No. 18, p. 467, 1984.

22. Bae, Y. K., M. J. Coggiola and J. R. Peterson: Observation of the Molecular Helium Negative Ion He_2^- . Physical Review Letters, 52, p. 747, 1984.

23. Michels, H. H.: Electronic Structure of the Helium Molecular Anion, He_2^- . Physical Review Letters, 52, p. 1413, 1984.

24. Hefter, U., R. D. Mead, P. A. Schulz and W. C. Lineberger: Ultrahigh-resolution study of autodetachment in C_2^- . Physical Review, A28, p. 1429, 1983.

25. Michels, H. H., R. H. Hobbs and L. A. Wright: Electronic Structure of the Lithium Molecular Anion, Li_2^- . Chemical Physics Letters, 118, p. 67, 1985.

26. Kvale, T. J., R. N. Compton, G. D. Alton, J. S. Thompson and D. J. Pegg: Autodetachment Spectroscopy of Metastable He_2^- . Physical Review Letters, 56, p. 592, 1986.

27. Ciocca, M., M. Allegrini, E. Arimondo, C. E. Burkhardt, W. P. Garver and J. J. Leventhal: Negative-Ion Formation in Rydberg-Atom Interactions (n = 7-40). Physical Review Letters, 56, p. 704, 1986.

REFERENCES (continued)

28. Cheret, M. and L. Barbier: Experimental Evidence for Negative–Ion Formation by the Collisional Reaction Rb(6d) + Rb(5s) → Rb$^+$ + Rb$^-$. Physical Review A $\underline{30}$, p. 1132, 1984.

29. McGeoch, M. and R. Schlier: abstract submitted to the 19th Annual Meeting of the Division of Atomic, Molecular and Optical Physics of the American Physical Society, Baltimore Maryland, April 18–20, 1988.

30. McGeoch, M. W.: A Dissociative Attachment Li$^-$ Source. AVCO/Everett Research Laboratory, work in progress.

31. Anderson, E. and J. Simons: A Calculation of the Electron Affinity of the Lithium Molecule. Journal of Chemical Physics, $\underline{64}$, p. 4548, 1976.

32. Dixon, D. A., J. L. Gole and K. D. Jordan: *Ab Initio* Study of the Electronic Structure of Li$_2^-$. Journal of Chemical Physics, $\underline{66}$, p. 567, 1977.

33. Rescigno, T. N.: *Electron–Molecule and Photon–Molecule Collisions.* Plenum Press, N.Y., 1979.

34. Truhlar, D. G.: *Resonances in Electron–Molecule Scattering.* ACS Symp. Series 263, 1984.

35. Miller, T. M., A. Kasdan and B. Bederson: Measurements of Total Cross Sections for Electron Scattering by Li$_2$ (0.5 – 10 eV). Phys. Rev. A, $\underline{25}$, p. 1777, 1982.

36. Teillet-Billy, D., L. Bouby and J. P. Ziesel: Abst 13th ICPEAC, ed, J. Eichler, et al., $\underline{294}$, 1983.

37. Nestmann, B. and S. D. Peyerimhoff: Calculations of the Discrete Component of Resonance States in Negative Ions by Variation of Nuclear Charges. J. Physics B, $\underline{18}$, p. 615, 1985.

38. Hiskes, J. R.: Cross Sections for the Vibrational Excitation of the H$_2$ (X$^1\Sigma_g^+$) State via Electron Collisional Excitation of the Higher Singlet States. Journal of Applied Physics, $\underline{51}$, p. 4592, 1980.

39. Nestmann, B. and S. D. Peyerimhoff: Calculation of the Discrete Component of Resonance States in Negative Ions by Variation of Nuclear Charges. J. Phys. B, $\underline{18}$, p. 615, 1985.

40. Foreman, P. B., P. K. Rol and K. P. Coffin: The Repulsive $^1\Sigma_g^+$ He$_2$ Potential Obtained from Total Cross Sections, Journal of Chemical Physics, $\underline{61}$, p. 1658, 1974.

41. Michels, H. H., R. H. Hobbs and J. R Peterson: Spectral Intensity of the Hopfield Helium Continuum: An Analysis of the Ground State Potential for He$_2$. Chemical Physics Letters, $\underline{134}$, p. 571, 1987.

REFERENCES (continued)

42. Huffman, R. E., J. C. Larrabee and D. Chambers: New Excitation Unit for Rare Gas Continua in the Vacuum Ultraviolet. Applied Optics, 4, p. 1145, 1965.

43. Bae, Y. K., J. R. Peterson, H. H. Michels and R. H. Hobbs: He_2^- [$^4\Pi_g$] $\rightarrow$ $He_2[X^1\Sigma^+]$ Autodetachment Energy Spectrum: Assessment of the He_2^- and He_2 Ground State Potentials. Physical Review A, 37, p. 2778, 1988.

44. Ferguson, E. E., F. C. Fehsenfeld and D. L. Albritton in *Gas Phase Ion Chemistry*, ed. M. T. Bowers, Academic Press, NY, 1979.

45. Mark, T. D. and A. W. Castleman, Jr., in Advances in Atomic and Molecular Physics, 20, p. 64, 1985.

46. *Proceedings of the Hydrogen Cluster Ion Group*, ed. J. T. Bahns, University of Dayton, 1986.

47. Beuhler, R. J., S. Ehrenson and L. Friedman: Hydrogen Cluster Ion Equilibria, Journal of Chemical Physics, 79, p. 5982, 1983.

48. Elford, M. T.: The Heat of Dissociation of H_5^+ Derived from Measurements of Ion Mobilities, Journal of Chemical Physics, 79, p. 5951, 1983.

49. Yamaguchi, Y., J. F. Gaw and H. F. Schaefer III: Molecular Clustering About a Positive Ion. Structure, Energetics and Vibrational Frequencies of the Protonated Hydrogen Clusters H_3^+, H_5^+, H_7^+ and H_9^+ . Journal of Chemical Physics, 78, p. 4074, 1983.

50. Yamaguchi, Y., J. F. Gaw, R. B. Remington and H. F. Schafer III: The H_5^+ Potential Energy Hypersurface. Characterization of Ten Distinct Energetically Low-Lying Stationary Points, Journal of Chemical Physics, 86, p. 5072, 1987.

51. Kirchner, N. J., J. R. Gilbert and M. T. Bowers: The First Experimental Observation of Stable H_4^+ Ions, Chemical Physics Letters, 106, p. 7, 1984.

52. Kirchner, N. J. and M. T. Bowers: An Experimental Study of the Formation and Reactivity of Ionic Hydrogen Clusters: The First Observation and Characterization of the Even Clusters H_4^+, H_6^+, H_8^+ and H_{10}^+. Journal of Chemical Physics, 86, p. 1301, 1987.

53. Bae, Y. K., M. S. Coggiola and J. R. Peterson: Search for H_2^-, H_3^- and Other Metastable Negative Ions, Physical Review A 29, p. 2888, 1984.

54. Sapse, A. M., M. T. Rayez-Meaume, J. C. Rayez and L. S. Massa: Ion-Induced Dipole H_n^- Clusters, Nature, 278, p. 332, 1979.

REFERENCES (continued)

55. Rayez, J. C., M.T. Rayez – Meaume and L. J. Massa: Theoretical Study of the H_3^- Cluster, Journal of Chemical Physics, 75, p. 5393, 1981.

56. Hirao, K. and S. Yamabe: Theoretical Study on the Structure and Stability of Hydrogen–Ion Clusters H_n^+ and H_n^- (n = 3, 5, 7, 9, 11, 13), Chemical Physics, 80, p. 237, 1983.

57. Chung, S., and C. C. Lin: Excitation of the Electronic States of the Nitrogen Molecule by Electron Impact. Physical Review, A6, p. 988, 1972.

58. Chung, S. and C. C. Lin: Electron Excitation of Electronic States of the CO Molecule. Physical Review, A6, p. 1954, 1974.

59. Chung, S., C. C. Lin and E. T. P. Lee: Dissociation of the Hydrogen Molecule by Electron Impact. Physical Review, A12, p. 1340, 1975.

60. Cartwright, D. C. and A. Kupperman: Electron–Impact Excitation Cross Section for the Two Lowest Triplet States of Molecular Hydrogen. Physical Review, 163, p. 86, 1967.

61. Cartwright, D. C.: Total Cross Sections for the Excitation of the Triplet States in Molecular Nitrogen. Physical Review, A2, p. 1331, 1970; Errata to this paper, Physical Review, A5, p. 1974, 1972.

62. Miller, K. J. and M. Krauss: Born Inelastic Differential Cross Sections in H_2. Journal of Chemical Physics, 47, p. 3754, 1967.

63. Khare, S. P. and B. L. Moiseiwisch: The Dissociation of Hydrogen Molecules by Electron Impact. Proceeding of Physical Society, 88, p. 605, 1966.

64. Khare, S. P.: Excitation of Hydrogen Molecule by Electron Impact III. Singlet–Triplet Excitations. Physical Review, 157, p. 107, 1967.

65. Schneider, B. I.: R–Matrix Theory for Electron–Molecule Collision Using Analytic Basis Set Expansions. II. Electron– H_2 Scattering in the Static–Exchange Model. Physical Review, A11, p. 1957, 1975.

66. Burke, P. G., I. Mackey and I. Shimamura: R–Matrix Theory of Electron–Molecule Scattering. Journal of Physics B: Atomic and Molecular Physics, 10, p. 2497, 1977.

67. Rescigno, T. N., C. W. McCurdy, Jr., V. McKoy and C. F. Bender: Low–Energy Electron–Impact Excitation of the Hydrogen Molecule. Physical Review, A13, p. 216, 1976.

68. Rescigno, T. N., C. W. McCurdy, Jr., and V. McKoy: Discrete–Basis–Set Approach to Nonspherical Scattering. II. Physical Review, A10, p. 2240, 1974; Low–Energy e^- – H_2 Elastic Cross Sections Using Discrete Basis Functions, Physical Review, A11, p. 825, 1975.

REFERENCES (continued)

69. Chung, S., and C. C. Lin: Application of the Close-Coupling Method to Excitation of Electronic States and Dissociation of H_2 by Electron Impact. Physical Review, A17, p. 1874, 1978.

70. Kendrick, S. and B. D. Buckley, Daresbury Lab. Dept. DL/SCI/TM22T, May 1980; C. J. Noble: Daresbury Lab. Report, DL/SCI/TM33T, November 1982.

71. Noble, C. J., P.G. Burke and S. Salvini: Low-Energy Scattering of Electrons by Diatomic Molecules. J. Phys. B: Atomic and Molecular Physics, 15, p. 3779, 1982.

72. Burke, P. G., C. J. Noble and S. Salvini: Electron Scattering by Nitrogen Molecules at Intermediate Energies. J. Phys. B. 16, p. L113, 1983.

73. Gailitis, M.: New Forms of Asymptotic Expansions for Wavefunctions of Charged-Particle Scattering. J. Phys. B, 9, p. 843, 1976.

74. Baluja, K. L., P. G. Burke and L. A. Morgan: R-Matrix Propagation Program for Solving Coupled Second Order Differential Equations. Comp. Phys. Commun. 27, p. 299, 1982.

75. Collins, L. A. and B. I. Schneider: Linear-Algebraic Approach to Electron-Molecule Collisions: General Formulation. Phys. Rev. A24, p. 2387, 1981.

76. Wadehra, J. M. and H. H. Michels: Vibrational Excitation of Li_2 $(X^1\Sigma_g^+)$ via Electron or Photon Excitation of the $A^1\Sigma_u^+$ and $B^1\Pi_u$ States. Chem. Phys. Lett. 114, p. 380, 1985.

77. Compton, R. N.: private communication.

78. Mittleman, M. H.: Resonant Laser Induced Negative Ion Production, Journal of Physics B: Atomic and Molecular Physics, 12, p. 1781, 1979.

79. Harris, F. E. and H. H. Michels: Expansion Techniques for Inelastic Scattering. Physical Review Letters, 22, p. 1036, 1969.

80. Nesbet, R.: Variational Methods in Electron-Atom Scattering Theory (Physics of Atoms and Molecules Serv.). Plenum Press, 1980.

81. Prelec, K. ed. Proceedings of the Third International Symposium on the Production and Neutralization of Negative Ions and Beams, AIP Conference Proceedings, 111, NY, 1984.

82. Bacal, M.: Volume Generation of H^- Ions in Plasmas, Physica Scipta, T2/2, p. 467, 1982.

83. Allan, M. and S. F. Wong: Effect of Vibrational and Rotational Excitation on Dissociative Attachment in Hydrogen, Physical Review Letters, 41, p. 1791, 1978.

REFERENCES (continued)

84. Wadehra, J. M. and J. N. Bardsley: Vibrational and Rotational – State Dependence of Dissociative Attachment in e – H_2 Collisions, Physical Review Letters, 41, p. 1795, 1978; Dissociative Attachment and Vibrational Excitation in Low–Energy Collisions of Electrons with H_2 and D_2, Physical Review A 20, p. 1398, 1979.

85. McGeoch, M. W. and R. E. Schlier in the Proceedings of the Third International Symposium on the Production and Neutralization of Negative Ions and Beams, AIP Conference Proceedings 111, p. 291, ed K. Prelec, NY, 1984; Dissociative Attachment in Optically Pumped Lithium Molecules, Physical Review, A33, p. 1078, 1986.

86. Hiskes, J. R.: Cross Sections for the Vibrational Excitation of the H_2 $(X^1\Sigma_g^+)$ State via Electron Collisional Excitation of the Higher Singlet States, Journal of Applied Physics, 51, p. 4592, 1980.

87. Wadehra, J. M. and H. H. Michels: Vibrational Excitation of Li_2 $(X^1\Sigma_g^+)$ via Electron or Photon Excitation of the $A^1\Sigma_u^+$ and $B^1\Pi_u$ States, Chemical Physics Letters, 114, p. 380, 1985.

88. Lee, Y. T. and B. H. Mahan: Photosensitized Ionization of Alkali–Metal Vapors, Journal of Chemical Physics, 42, p. 2893, 1965 and references therein.

89. Bae, Y. K. and J. R. Peterson; Effect of a Virtual State Near an s–wave Threshold: Absolute Li^- Photodetachment Cross Sections Near the $Li(2^2P)$ Threshold, Physical Review A 32, p. 1917, 1985.

90. Wadehra, J. M., *Nonequilibrium Vibrational Kinetics*, ed. M. Capitelli, Springer–Verlag, Heidelberg, p. 191, 1986.

91. Gauyacq, J. P., *Dynamics of Negative Ions*, World Scientific, Singapore, 1987.

92. Bardsley, J. N., A. Herzenberg and F. Mandl, *Proceedings of the Third International Conference on Atomic Collisions*, North–Holland, Amsterdam, p. 415, 1964.

93. Harris, F. E. and H. H. Michels: Open–Shell Valence Configuration–Interaction Studies of Diatomic and Polyatomic Molecules, International Journal of Quantum Chemistry, IS, p. 329, 1967.

94. Nestmann, B. and S. D. Peyerimhoff: Calculation of the Discrete Component of Resonance States In Negative Ions by Variation of Nuclear Charges, Journal of Physics B, 18, p. 615, 1985.

95. Krishnan, R., J. S. Binkley, R. Seeger and J. A. Pople: Self–consistent Molecular Orbital Methods. XX. A Basis Set for Correlated Wave Functions, Journal of Chemical Physics, 72, p. 650, 1980.

REFERENCES (continued)

96. Amos, R. D. and J. E. Rice, CADPAC: The Cambridge Analytic Derivatives Package–Issue 4.0, Cambridge, 1987.

97. Jordan, K. D., K. M. Griffing, J. Kenney, E. L. Andersen and J. Simons: Theoretical Study of Stable Negative Ions of Polar Molecules: NaH^-, LiH^-, LiF^-, BeO^-, Journal of Chemical Physics, 64, p. 4730, 1976.

98. Cardelino, B. H., W. H. Eberhardt and R. F. Borkman; *Ab initio* SCF Calculation on Li_nH_m Molecules and Cations with Four or Less Atoms, Journal of Chemical Physics, 84, p. 3230, 1986.

99. Montgomery, J. A., H. H. Michels, O. F. Güner and K. Lammertsma: The Structure and Bonding of Li_3H Ion–Pair States, Chemical Physics Letters, 161, p. 291, 1989.

100. Wodtke, A. M. and Y. T. Lee: Photodissociation of Acetylene at 193.3 nm, Journal of Physical Chemistry, 89, p. 4744, 1985.

101. Shiromaru, H., Y. Achiba, K. Kimura and Y. T. Lee: Determination of the C–H Bond Dissociation Energies of Ethylene and Acetylene by Observation of the Threshold Energies of H^+ Formation by Synchrotron Radiation, Journal of Physical Chemistry, 91, p. 17, 1987.

102. Fujii, M., A. Haijima and M. Ito: Predissociation of Acetylene in $\bar{A}$ ^1A_u State, Chemical Physics Letters, 150, p. 380, 1988.

103. Curtiss, L. A. and J. A. Pople: Theoretical Study of the C–H Bond Dissociation Energy of Acetylene, Journal of Chemical Physics, 91, p. 2420, 1989.

104. Green, P. G., J. L. Kinsey and R. W. Field: A New Determination of the Dissociation Energy of Acetylene, Journal of Chemical Physics, 91, p. 5160, 1989.

105. Segall, J., R. Lavi, Y. Wen and C. Wittig: Acetylene C–H Bond Dissociation Energy Using 193.3–nm Photolysis and Sub–Doppler Resolution H–Atom Spectroscopy: 127 ± 1.5 k cal/mol, Journal of Physical Chemistry, 93, p. 7287, 1989.

106. S. W. Benson, as quoted by Segall, et al. (Ref. 105)

107. Nyden, M. R. and G. A. Petersson: Complete Basis Set Correlation Energies. I. The Asymptotic Convergence of Pair Natural Orbital Expansion, Journal of Chemical Physics, 75, p. 1843, 1981.

108. Petersson, G. A. and M. R. Nyden: Interference Effects in Pair Correlation Energies: Helium L–limit Energies, Journal of Chemical Physics, 75, p. 3423, 1981.

109. Petersson, G. A. and S. L. Licht: Complete Basis Set Correlation Energies. II. The Beryllium Isoelectronic Series, Journal of Chemical Physics, 75, p. 4556, 1981.

REFERENCES (continued)

110. Petersson, G. A., A. K. Yee and A. Bennett: Complete Basis Set Correlation Energies. III. The Total Correlation Energy of the Neon Atom, Journal of Chemical Physics, 83, p. 5105, 1985.

111. Petersson, G. A. and M. Braunstein: Complete Basis Set Correlation Energies. IV. The Total Correlation Energy of the Water Molecule, Journal of Chemical Physics, 83, p. 5129, 1985.

112. Petersson, G. A., A. Bennett, T. G. Tensfeldt, M. A. Al-Laham and W. A. Shirley: A Complete Basis Set Model Chemistry. I. The Total Energies of Closed-shell Atoms and Hydrides of the First-row Elements, Journal of Chemical Physics, 89, p. 2193, 1988.

113. Petersson, G. A. and M. A. Al-Laham: Heat of Formation of Singlet Methylene, Journal of the American Chemical Society, 111, p. 1256, 1989.

114. Montgomery, J. A., G. A. Petersson and N. Matsunaga: On the Helium Pair Potential, Chemical Physics Letters, 155, p. 413, 1989.

115. Petersson, G. A. and W. A. Shirley: The Beryllium Dimer Potential, Chemical Physics Letters, 160, p. 494, 1989.

116. Ervin, K. M., S. Gronert, S. E. Barlow, M. K. Gilles, A. G. Harrison, V. M. Bierbaum, C. H. DePuy, W. C. Lineberger, and G. B. Ellison: Bond Strengths of Ethylene and Acetylene, Journal of the American Chemical Society, 112, p. 5750, 1990.

117. Ervin, K. M. and W. C. Lineberger: Photoelectron Spectra of C_2^- and C_2H^-, Journal of Physical Chemistry, 95, p. 1167, 1991.

118. Huber, K. P. and G. Herzberg: Abstracts of Diatomic Molecules, van Nostrand Reinhold, NY, 1979.

119. Ervin, K. M., J. Ho and W. C. Lineberger: A Study of the Singlet and Triplet States of Vinylidene by Photoelectron Spectroscopy of $H_2C = C^-$, $D_2C = C^-$ and $HDC = C^-$. Vinylidene-acetylene Isomerization, Journal of Chemical Physics, 91, p. 5974, 1989.

120. Hammond, G. S.: A Correlation of Reaction Rates, Journal of the American Chemical Society, 77, p. 334, 1955.

TABLE 1

Calculated Electronic Energies and Bond Lengths for H_3^-.

Level	R_1	R_2	H_3^- electronic energy	H_3^- zero-pt. energy	H^- electronic energy	H_2 electronic energy	H_2 zero-pt. energy	D_e	D_o
SCF/small	0.7340	3.2120	-1.621341	0.01250	-0.487640	-1.132408	0.01046	1.29	-0.75
MP2/small	0.7451	2.8977	-1.668994	0.01277	-0.507128	-1.160181	0.01030	1.68	-0.79
MP4/small	0.7482	2.9607	-1.683973	---	-0.514803	-1.167750	---	1.42	---
CISD/small	0.7480	3.0933	-1.684610	0.01227	-0.517166	-1.168354	0.01005	1.25	-0.97
SCF/large	0.7385	3.2020	-1.622682	0.01236	-0.487785	-1.133502	0.01046	1.40	-0.50
MP2/large	0.7436	2.8129	-1.679633	0.01258	-0.514177	-1.163478	0.01032	1.98	-0.28
MP4/large	0.7473	2.8950	-1.697126	---	-0.524534	-1.170956	---	1.64	---
CISD/large	0.7469	2.9583	-1.696702	0.01216	-0.526268	-1.171560	0.01005	1.58	-0.53
SCF/huge	0.7383	3.2015	-1.622877	0.01234	-0.487887	-1.133598	0.01044	1.39	-0.51
MP2/huge	0.7438	2.7649	-1.682973	0.01257	-0.515161	-1.165762	0.01031	2.05	-0.21
MP4/huge	0.7476	2.8695	-1.699551	---	-0.524995	-1.172764	---	1.79	---
CISD/huge	0.7476	2.8695	-1.698957	---	-0.526727	-1.173376	0.01005		

Bond lengths are in angstroms, energies in hartrees,
except D_e and D_o, which are in millihartrees. R_1 is the H – H
equilibrium separation, and R_2 is the H_2 – H^- equilibrium separation.

As CISD is not size-consistent, the CISD D_e values are found from
$D_e(CISD) = E[R_1=H_2(R_e), R_2=15\text{Å}] - E[eq]$. $D_o = D_e - ZPE(H_3^-) + ZPE(H_2)$.

41

TABLE 2

LOW-LYING MOLECULAR STATES OF Li_2 AND THEIR DISSOCIATION LIMITS

Separated atoms	E(cm^{-1})[*]	Molecular states
Li + Li		
$^2S_g(2s)$ + $^2S_g(2s)$	0.0	$^1\Sigma_g^+(1)$, $^3\Sigma_u^+(1)$
$^2S_g(2s)$ + $^2P_u(2p)$	14903.0	$^1\Sigma_g^+(1)$, $^1\Sigma_u^+(1)$, $^3\Sigma_g^+(1)$, $^3\Sigma_u^+(1)$
		$^1\Pi_g(1)$, $^1\Pi_u(1)$, $^3\Pi_g(1)$, $^3\Pi_u(1)$
$^2S_g(2s)$ + $^2S_g(3s)$	27206.0	$^1\Sigma_g^+(1)$, $^1\Sigma_u^+(1)$, $^3\Sigma_g^+(1)$, $^3\Sigma_u^+(1)$
$^2P_u(2p)$ + $^2P_u(2p)$	29807.0	$^1\Sigma_g^+(2)$, $^1\Sigma_u^-(1)$, $^3\Sigma_u^+(2)$, $^3\Sigma_g^-(1)$
		$^1\Pi_g(1)$, $^1\Pi_u(1)$, $^3\Pi_g(1)$, $^3\Pi_u(1)$
		$^1\Delta_g(1)$, $^3\Delta_u(1)$,
$^2S_g(2s)$ + $^2P_u(3p)$	30925.0	$^1\Sigma_g^+(1)$, $^1\Sigma_u^+(1)$, $^3\Sigma_g^+(1)$,
		$^3\Sigma_u^+(1)$, $^1\Pi_g(1)$, $^1\Pi_u(1)$,
		$^3\Pi_g(1)$, $^3\Pi_u(1)$
$^2S_g(2s)$ + $^2D_g(3d)$	31283.0	$^1\Sigma_g^+(1)$, $^1\Sigma_u^+(1)$, $^3\Sigma_g^+(1)$,
		$^3\Sigma_u^+(1)$, $^1\Pi_g(1)$, $^1\Pi_u(1)$, $^3\Pi_g(1)$,
		$^3\Pi_u(1)$, $^1\Delta_g(1)$, $^1\Delta_u(1)$, $^3\Delta_g(1)$,
		$^3\Delta_u(1)$
$Li_2^+[^2\Sigma_u^+]$ + e	33200.0	
$^2S_g(2s)$ + $^2S_g(4s)$	35012.0	$^1\Sigma_g^+(1)$, $^1\Sigma_u^+(1)$, $^3\Sigma_g^+(1)$, $^3\Sigma_u^+(1)$
$^2S_g(2s)$ + $^2P_u(4p)$	36469.0	$^1\Sigma_g^+(1)$, $^1\Sigma_u^+(1)$, $^3\Sigma_g^+(1)$,
		$^3\Sigma_u^+(1)$, $^1\Pi_g(1)$, $^1\Pi_u(1)$,
		$^3\Pi_g(1)$, $^3\Pi_u(1)$

[*]C. E. Moore, Atomic Energy Levels, 1, 9 (1949).

TABLE 2 (Continued)

$^2S_g(2s)$ + $^2D_g(4d)$	36623.0	$^1\Sigma_g^+(1)$, $^1\Sigma_u^+(1)$, $^3\Sigma_g^+(1)$,
		$^3\Sigma_u^+(1)$, $^1\Pi_g(1)$, $^1\Pi_u(1)$, $^3\Pi_g(1)$,
		$^3\Pi_u(1)$, $^1\Delta_g(1)$, $^1\Delta_u(1)$, $^3\Delta_g(1)$,
		$^3\Delta_u(1)$
$^2S_g(2s)$ + $^2F_u(4f)$	36630.0	$^1\Sigma_g^+(1)$, $^1\Sigma_u^+(1)$, $^3\Sigma_g^+(1)$,
		$^3\Sigma_u^+(1)$, $^1\Pi_g(1)$, $^1\Pi_u(1)$, $^3\Pi_g(1)$,
		$^3\Pi_u(1)$, $^1\Delta_g(1)$, $^1\Delta_u(1)$, $^3\Delta_g(1)$,
		$^3\Delta_u(1)$, $^1\Phi_g(1)$, $^1\Phi_u(1)$, $^3\Phi_g(1)$,
		$^3\Phi_u(1)$
$^2S_g(2s)$ + $^2S_g(5s)$	38299.0	$^1\Sigma_g^+(1)$, $^1\Sigma_u^+(1)$, $^3\Sigma_g^+(1)$, $^3\Sigma_u^+(1)$
Li$^+$ [$^1S_g(1s^2)$] + Li$^-$ [$^1S_g(2s^2)$]	38474.0	$^1\Sigma_g^+(1)$, $^1\Sigma_u^+(1)$
$^2S_g(2s)$ + $^2P_u(5p)$	39015.0	$^1\Sigma_g^+(1)$, $^1\Sigma_u^+(1)$, $^3\Sigma_g^+(1)$,
		$^3\Sigma_u^+(1)$, $^1\Pi_g(1)$, $^1\Pi_u(1)$, $^3\Pi_g(1)$,
		$^3\Pi_u(1)$
$^2S_g(2s)$ + $^2D_g(5d)$	39094.0	$^1\Sigma_g^+(1)$, $^1\Sigma_u^+(1)$, $^3\Sigma_g^+(1)$,
		$^3\Sigma_u^+(1)$, $^1\Pi_g(1)$, $^1\Pi_u(1)$, $^3\Pi_g(1)$,
		$^3\Pi_u(1)$, $^1\Delta_g(1)$, $^1\Delta_u(1)$, $^3\Delta_g(1)$,
		$^3\Delta_u(1)$
$^2S_g(2s)$ + $^2F_u(5f)$	39104.0	$^1\Sigma_g^+(1)$, $^1\Sigma_u^+(1)$, $^3\Sigma_g^+(1)$, $^3\Sigma_u^+(1)$,
		$^1\Pi_g(1)$, $^1\Pi_u(1)$, $^3\Pi_g(1)$, $^3\Pi_u(1)$,
		$^1\Delta_g(1)$, $^1\Delta_u(1)$, $^3\Delta_g(1)$, $^3\Delta_u(1)$,
		$^1\Phi_g(1)$, $^1\Phi_u(1)$, $^3\Phi_g(1)$, $^3\Phi_u(1)$
$^2S_g(2s)$ + Doublets $(5<n\overset{\sim}{<}9)$	39987.0 + 42003.0	Singlet, triplet Σ, Π, Δ, (g,u)

43

TABLE 2 (Concluded)

$^2P_u(2p)$ + $^2S_g(3s)$	42110.0	$^1\Sigma_g^+(1)$, $^1\Sigma_u^+(1)$, $^3\Sigma_g^+(1)$, $^3\Sigma_u^+(1)$, $^1\Pi_g(1)$, $^1\Pi_u(1)$, $^3\Pi_g(1)$, $^3\Pi_u(1)$
$^2S_g(2s)$ + Doublet $(9 \leq n \leq \infty)$	42118.0 →	Singlet, triplet Σ, Π, Δ (g,u)
Li^+ [$^1S_g(1s^2)$] + Li [$^2S_g(2s)$]	43482.0	$^2\Sigma_g^+(1)$, $^2\Sigma_u^+(1)$
$^2P_u(2p)$ + $^2P_u(3p)$	45829.0	$^1\Sigma_g^+(2)$, $^1\Sigma_u^+(2)$, $^3\Sigma_g^+(2)$, $^3\Sigma_u^+(2)$, $^1\Sigma_g^-(1)$, $^1\Sigma_u^-(1)$, $^3\Sigma_g^-(1)$, $^3\Sigma_u^-(1)$, $^1\Pi_g(2)$, $^1\Pi_u(2)$, $^3\Pi_g(2)$, $^3\Pi_u(2)$, $^1\Delta_g(1)$, $^1\Delta_u(1)$, $^3\Delta_g(1)$, $^3\Delta_u(1)$
$^2P_u(2p)$ + $^2D_g(3d)$	46187.0	$^1\Sigma_g^+(2)$, $^1\Sigma_u^+(2)$, $^1\Sigma_g^-(1)$, $^1\Sigma_u^-(1)$, $^3\Sigma_g^+(2)$, $^3\Sigma_u^+(2)$, $^3\Sigma_g^-(1)$, $^3\Sigma_u^-(1)$, $^1\Pi_g(3)$, $^1\Pi_u(3)$, $^3\Pi_g(3)$, $^3\Pi_u(3)$, $^1\Delta_g(2)$, $^1\Delta_u(2)$, $^3\Delta_g(2)$, $^3\Delta_u(2)$ $^1\Phi_g(1)$, $^1\Phi_u(1)$, $^3\Phi_g(1)$, $^3\Phi_u(1)$
$^2P_u(2p)$ + Doublet $(n=4, 5)$	51088.0 → 53782.0	Singlet, triplet Σ, Π, Δ, Φ, Γ (g,u)
$^2S_g(3s)$ + $^2S_g(3s)$	54412.0	$^1\Sigma_g^+(1)$, $^3\Sigma_u^+(1)$
Li^+ [$^1S_g(1s^2)$] + Li^- [$^1P_u(2s2p)$]	57920.0	$^1\Sigma_g^+(1)$, $^1\Sigma_u^+(1)$, $^1\Pi_g(1)$, $^1\Pi_u(1)$

TABLE 3
THERMODYNAMICS OF Li_xH_y CLUSTERS

Reaction	ΔE (eV)	
Li_2 (g) + H_2 (g) → 2LiH (g)	+0.740	(1)
Li_2 (g) + 1/2 H_2 (g) → Li_2H (C_{2v})	–0.280	(2)
3/2 Li_2 (g) + 1/2 H_2 (g) → Li_3H (C_{2v})	–1.034	(3)
Li_2 (g) + H_2 (g) → Li_2H_2 (D_{2h})	–1.263	(4)

FIG. 1

Potential energy curves of Li_2^-

82-3-121-1
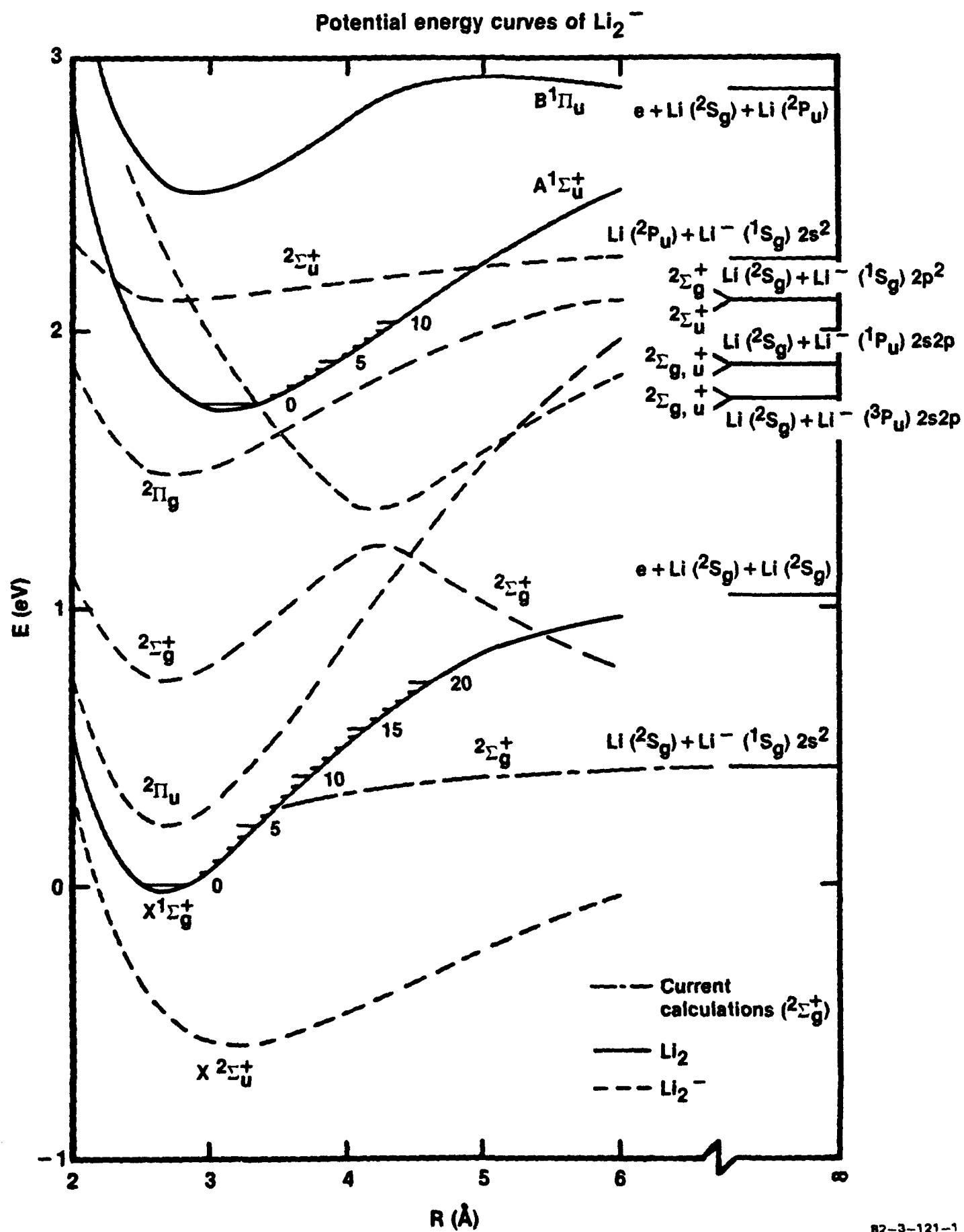
Low-Lying Potential Energy Curves of Li_2^-

DISSOCIATIVE ELECTRON ATTACHMENT CROSS SECTION FOR e + Li$_2$ [X $^1\Sigma_g^+$]

FIG. 4
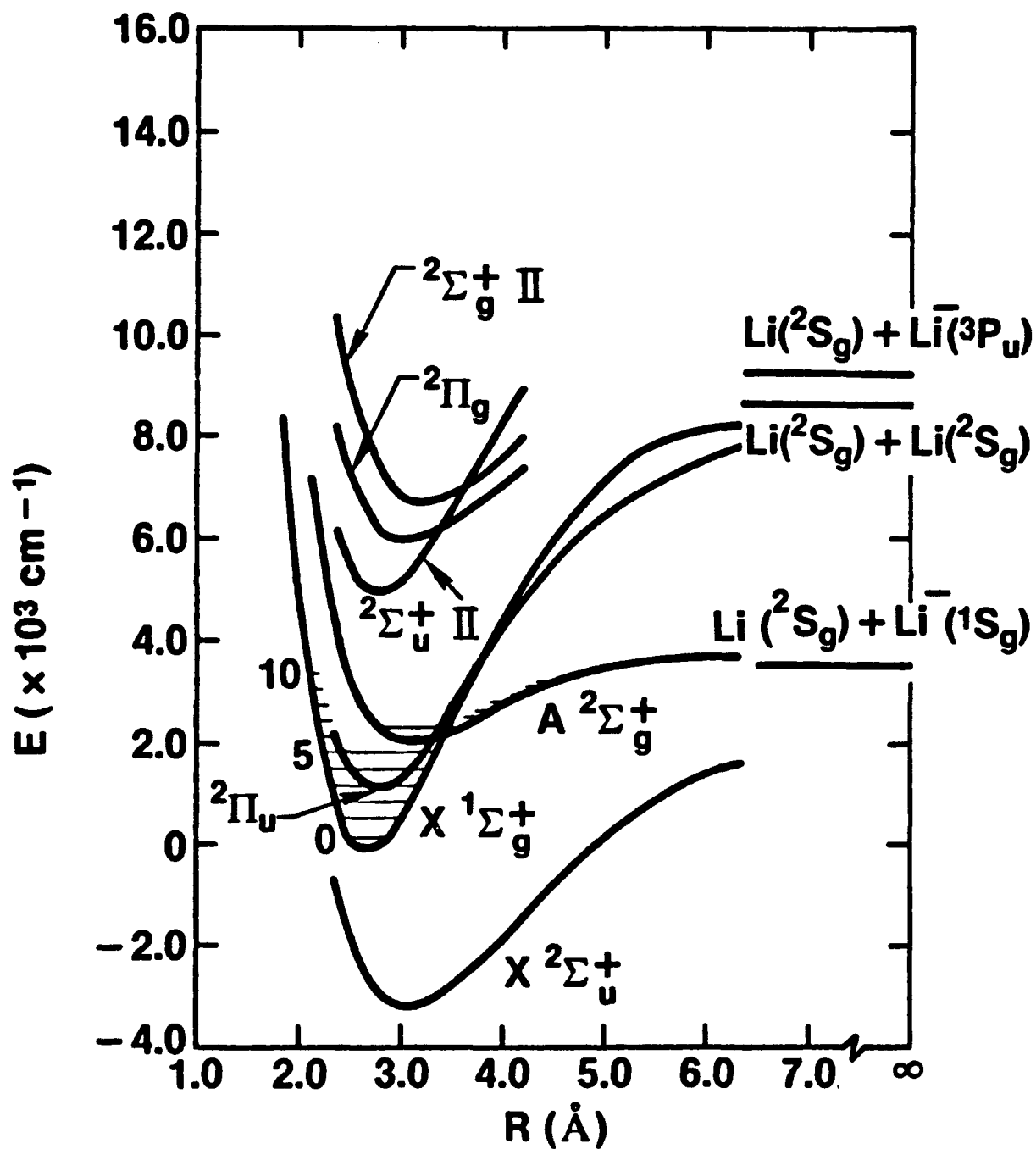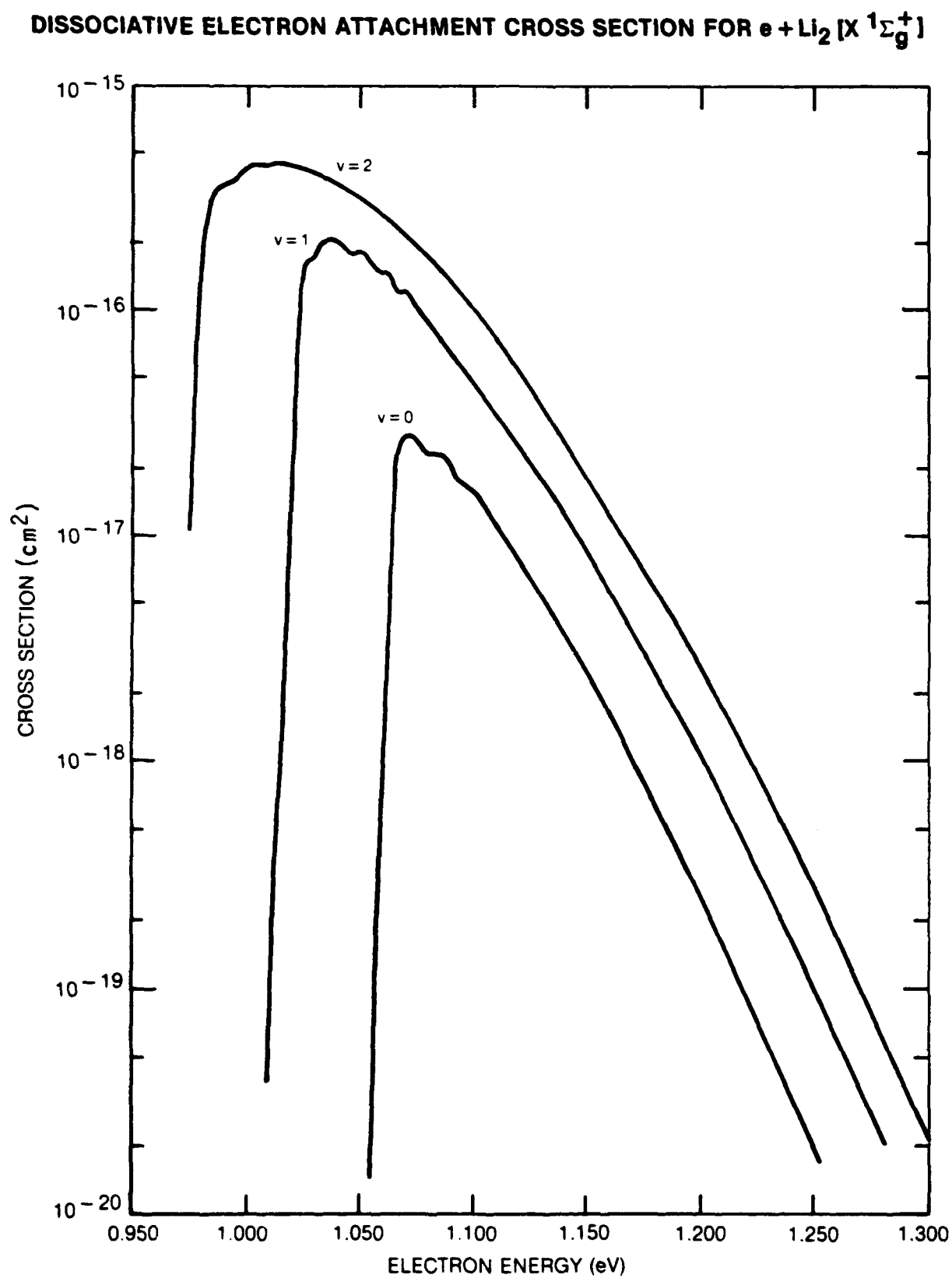
POTENTIAL ENERGY CURVES FOR He_2 AND He_2^-

$He + He$

$^1S_g + ^3P_u$

$^1S_g + ^3S_g$

$^1S_g + ^4P_u$

$b^3\Pi_g$

$^4\Pi_g$

$a^3\Sigma_u^+$

He_2 ——

He_2^- – – –

$^4\Sigma_g^+$ ○

$^4\Sigma_u^+$ □

$^4\Pi_u$ △

$R(\text{Å})$

$E\ (\times 10^3\ cm^{-1})$

170
166
162
158
154
150
146
142

0   0.4   0.8   1.2   1.6   2.0   2.4   2.8   3.2   3.6   ∞
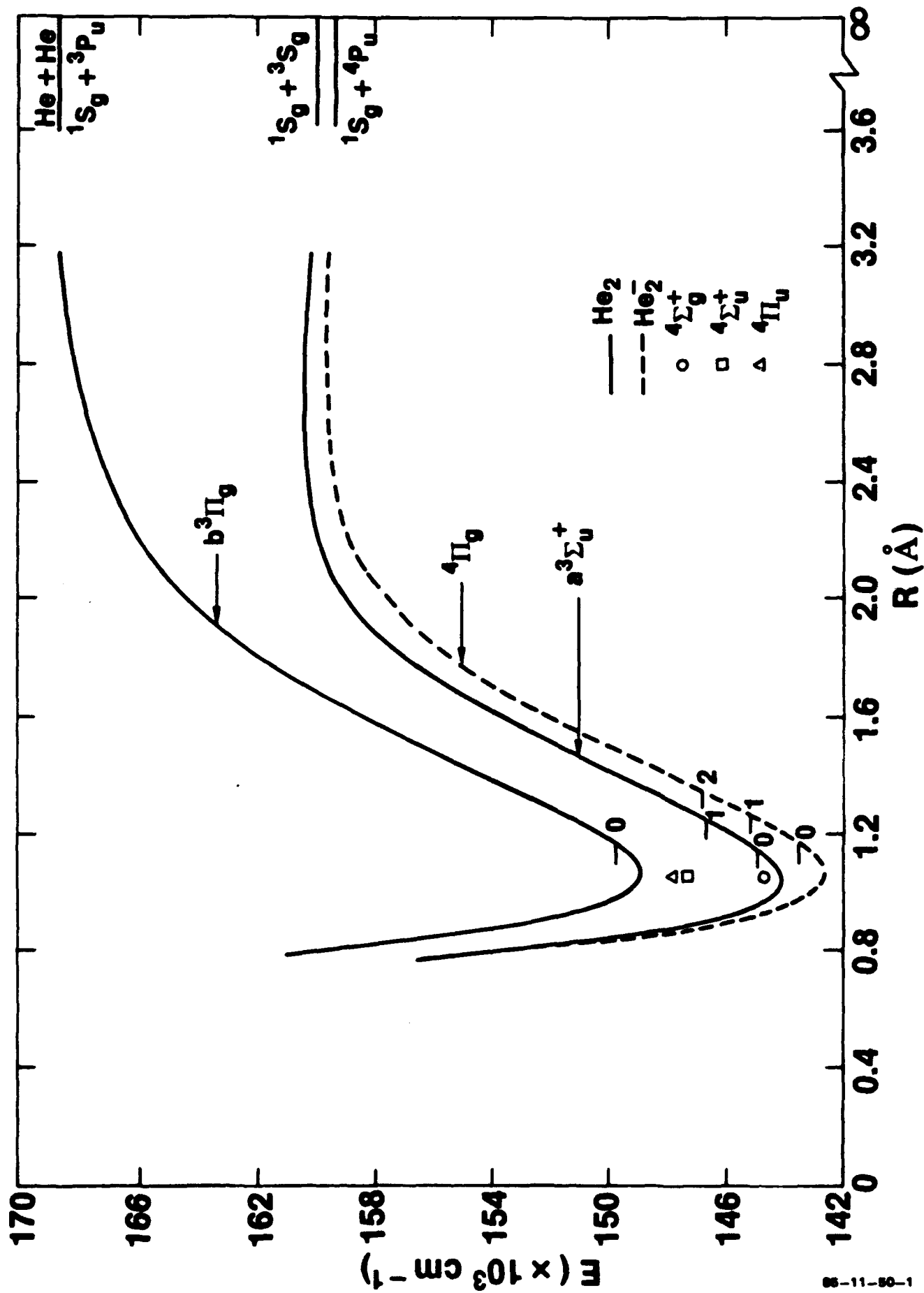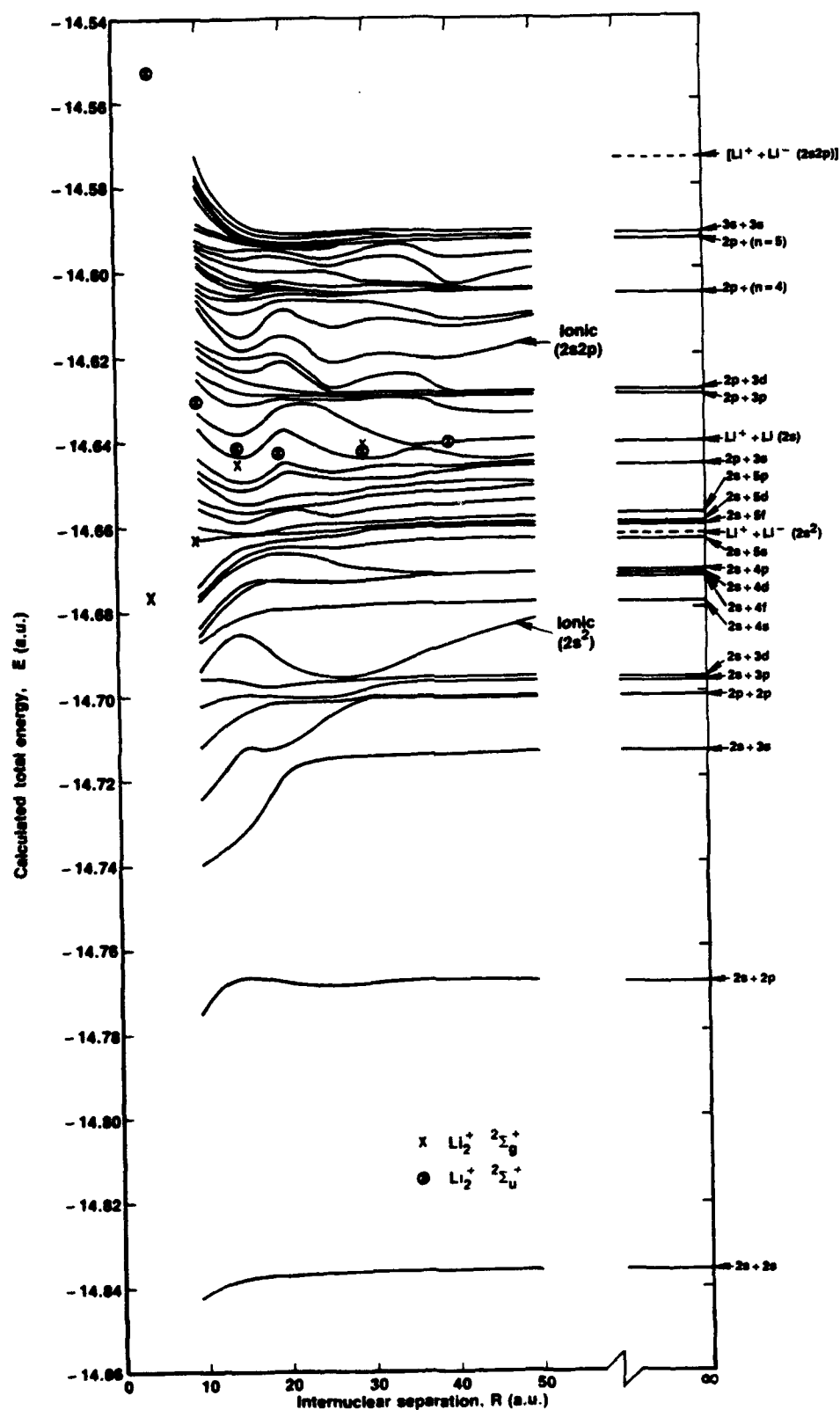
Fig. 1 Long-range behavior of excited $^1\Sigma_g^+$ states of Li$_2$.

FIG. 6
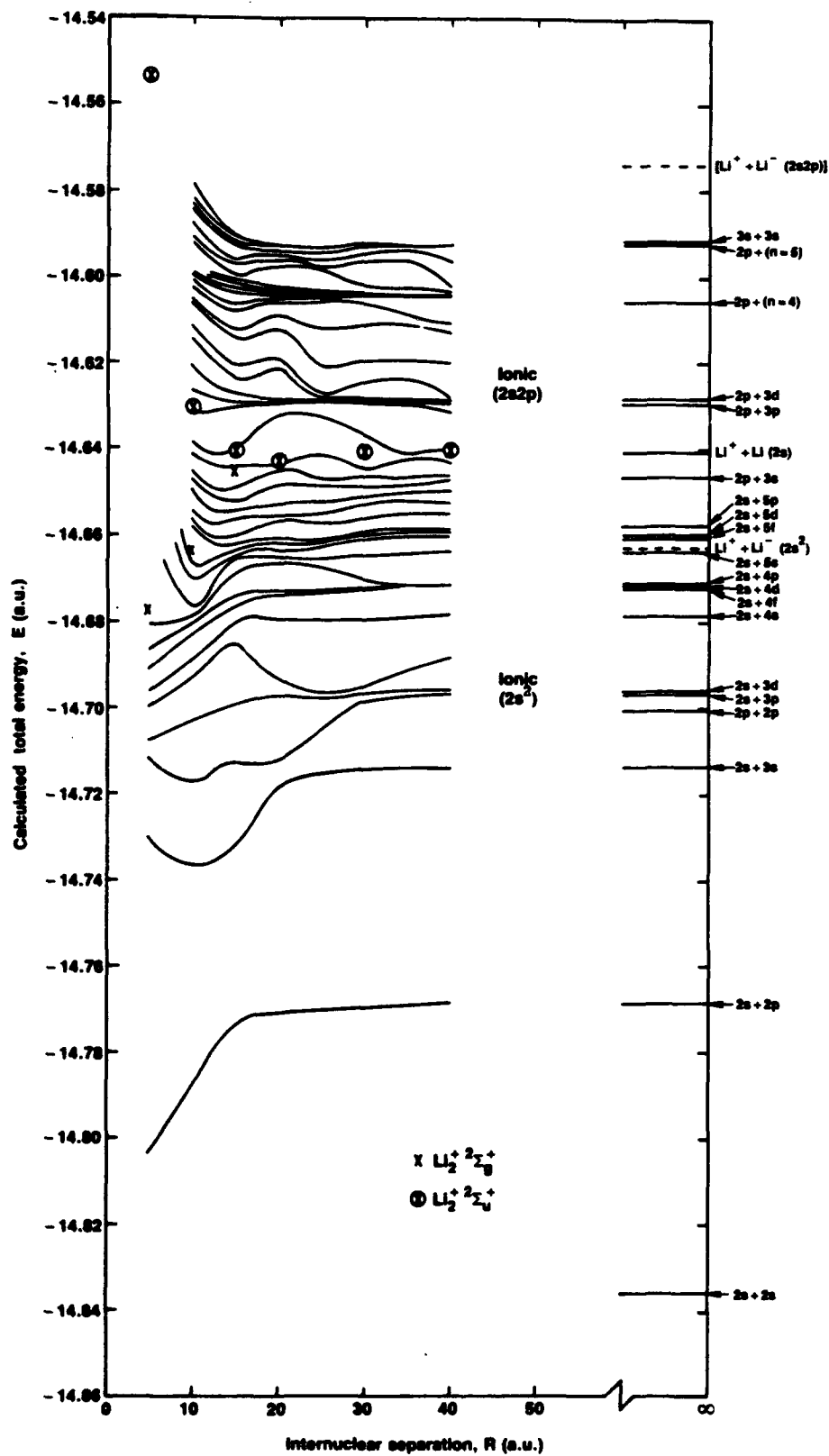
Fig. 2 Long-range behavior of excited $^1\Sigma_u^+$ states of Li$_2$.

FIG. 7

LiH/LiH⁻ POTENTIAL ENERGY CURVES
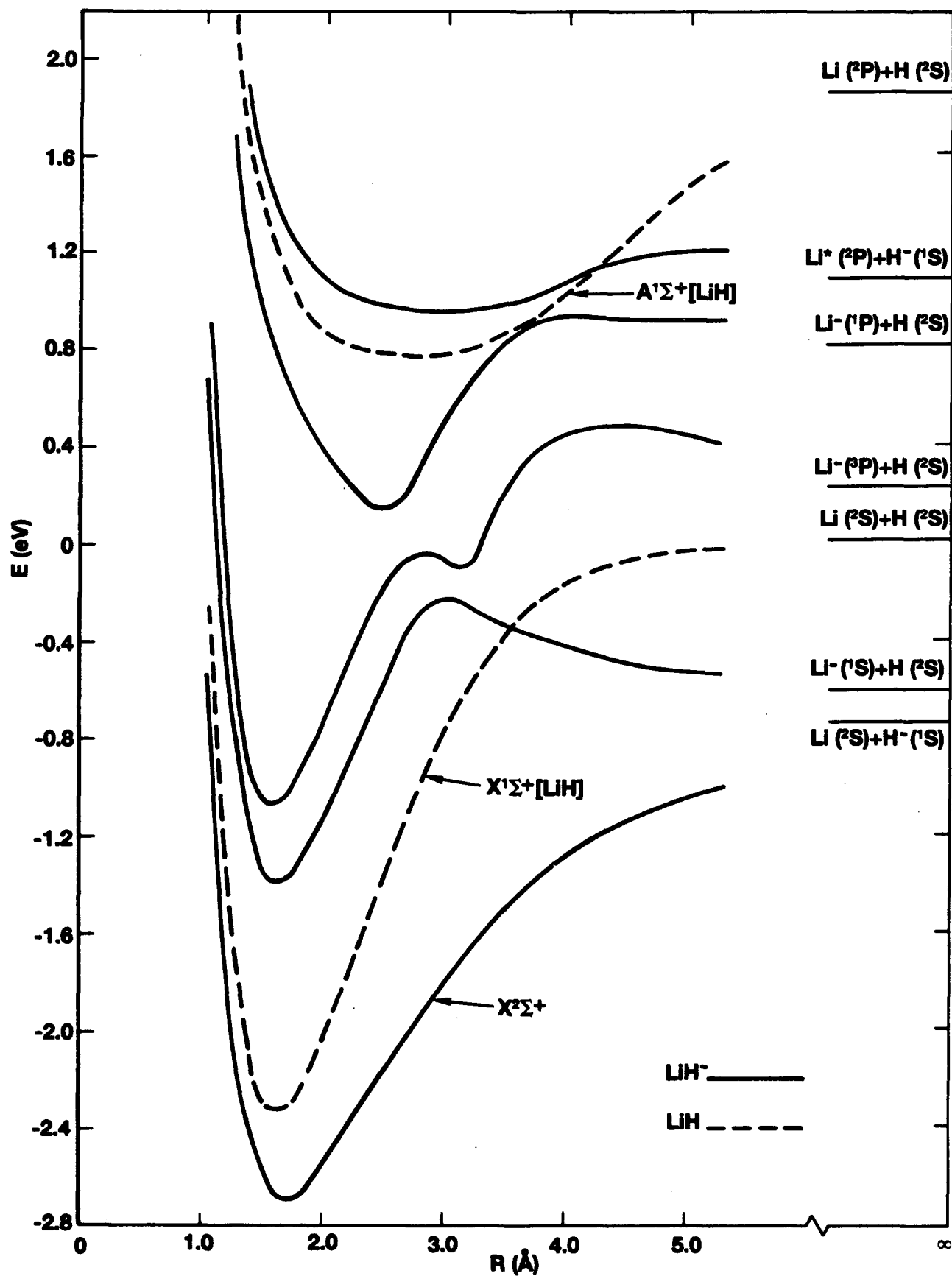
89-10-40-1

SHORT RANGE INTERACTION POTENTIALS FOR LiH/LiH⁻

88—5—13—3
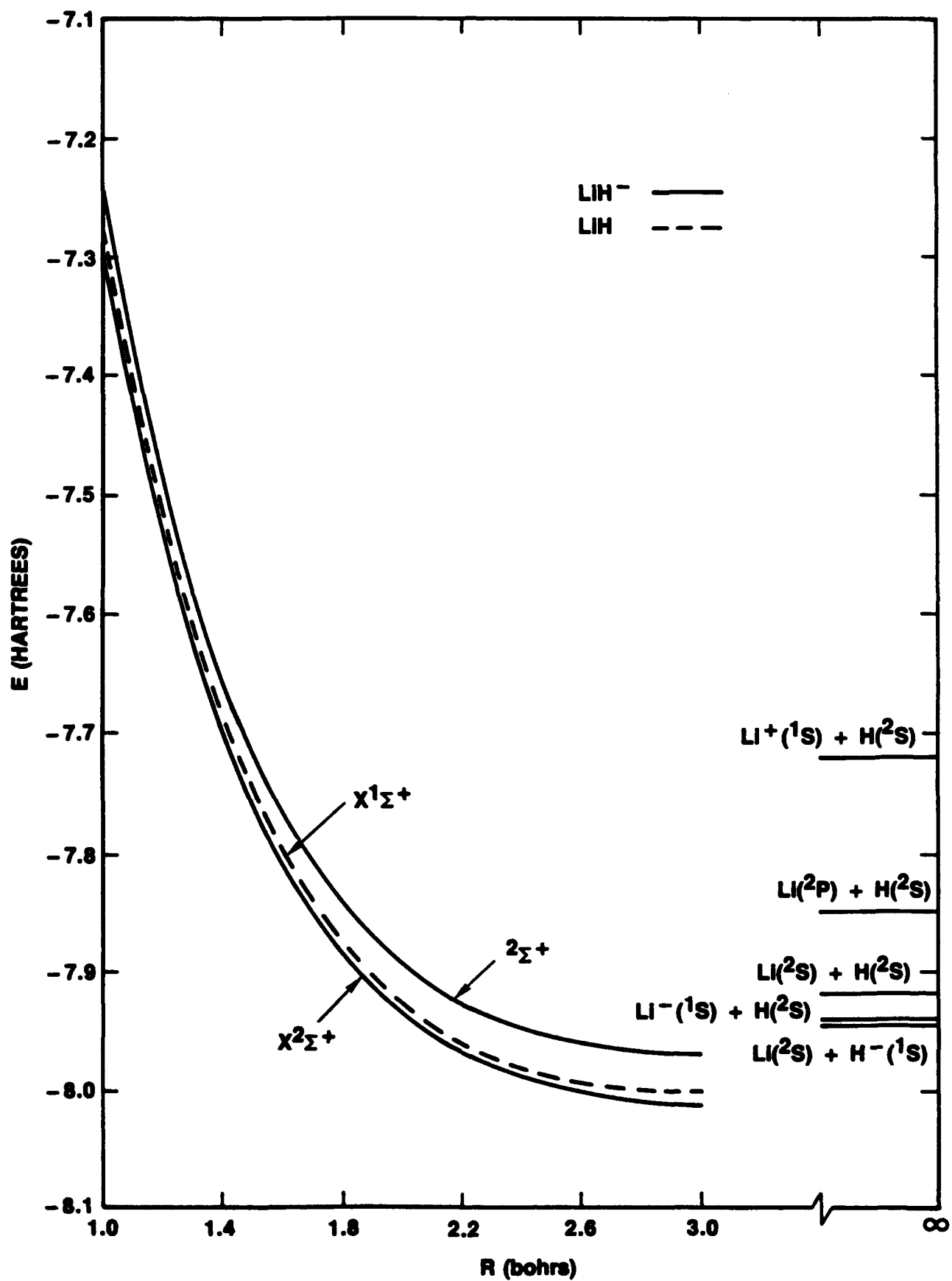
POTENTIAL ENERGY CURVES OF H_2, LiH, Li_2 AND THEIR ANIONS

Li₂H / Li₂H⁻ STRUCTURES

Li₂H

Li 94.3°

1.71

Li H

C₂ᵥ

stable structure

Li₂H⁻

Li 102.5°

1.71

Li H
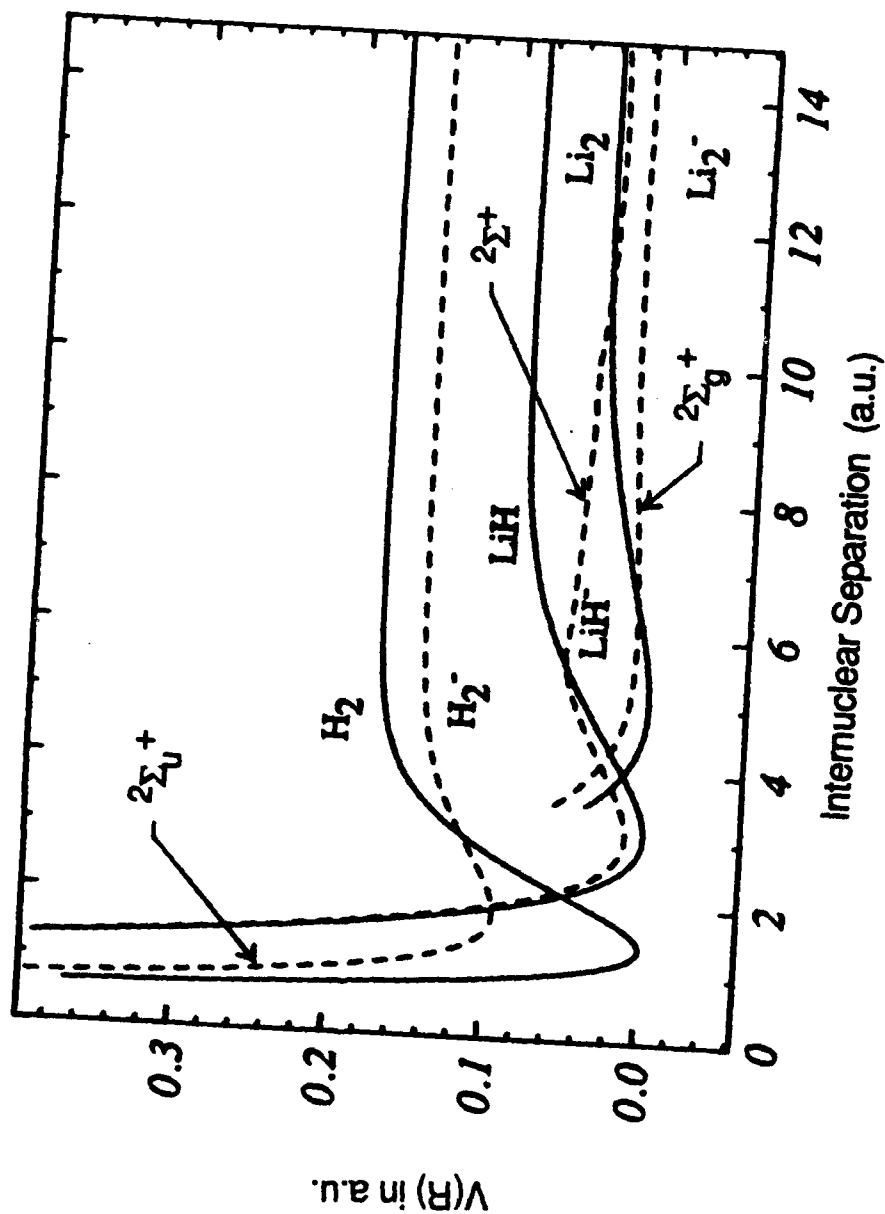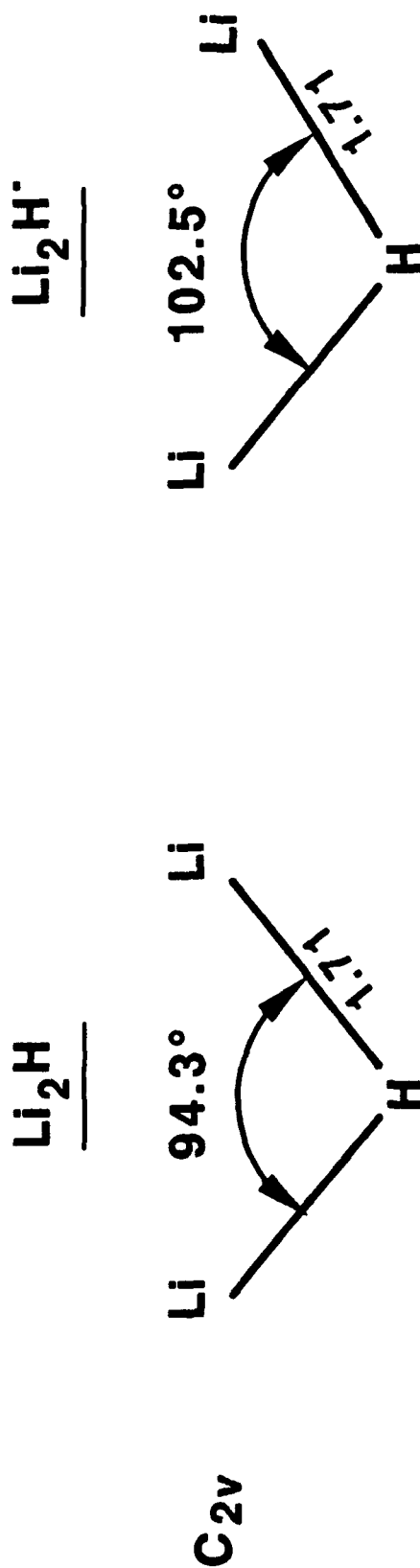
**bound by 0.06 eV
relative to neutral (C₂ᵥ)**

FIG. 11

Li₃H/Li₃H⁻ STRUCTURES

FIG. 12

$Li_2H_2 / Li_2H_2^-$ STRUCTURES

Li_2H_2

$Li^{1.58}{}_H{}^{1.75}{}_{Li}{}^{1.64}{}_H$

$\mu = 13.7$ debye

saddle pt.: 1 imag. freq.

Linear
($C_{\infty v}$)

Rhomboid
(D_{2h})

2.67

1.75

80.3°

stable sructure

Y - structure
(C_{2v})

unstable $\longrightarrow$ $Li_2 + H_2$

$Li_2H_2^-$

$Li^{1.60}{}_H{}^{1.73}{}_{Li}{}^{1.67}{}_H$

unbound by 0.040 eV
relative to neutral ($C_{\infty v}$)

2.69

1.76

80.8°

unbound by 2.05 eV
relative to neutral (D_{2h})

4.88

2.96

0.77

unbound by 1.50 eV
relative to neutral (D_{2h})

57
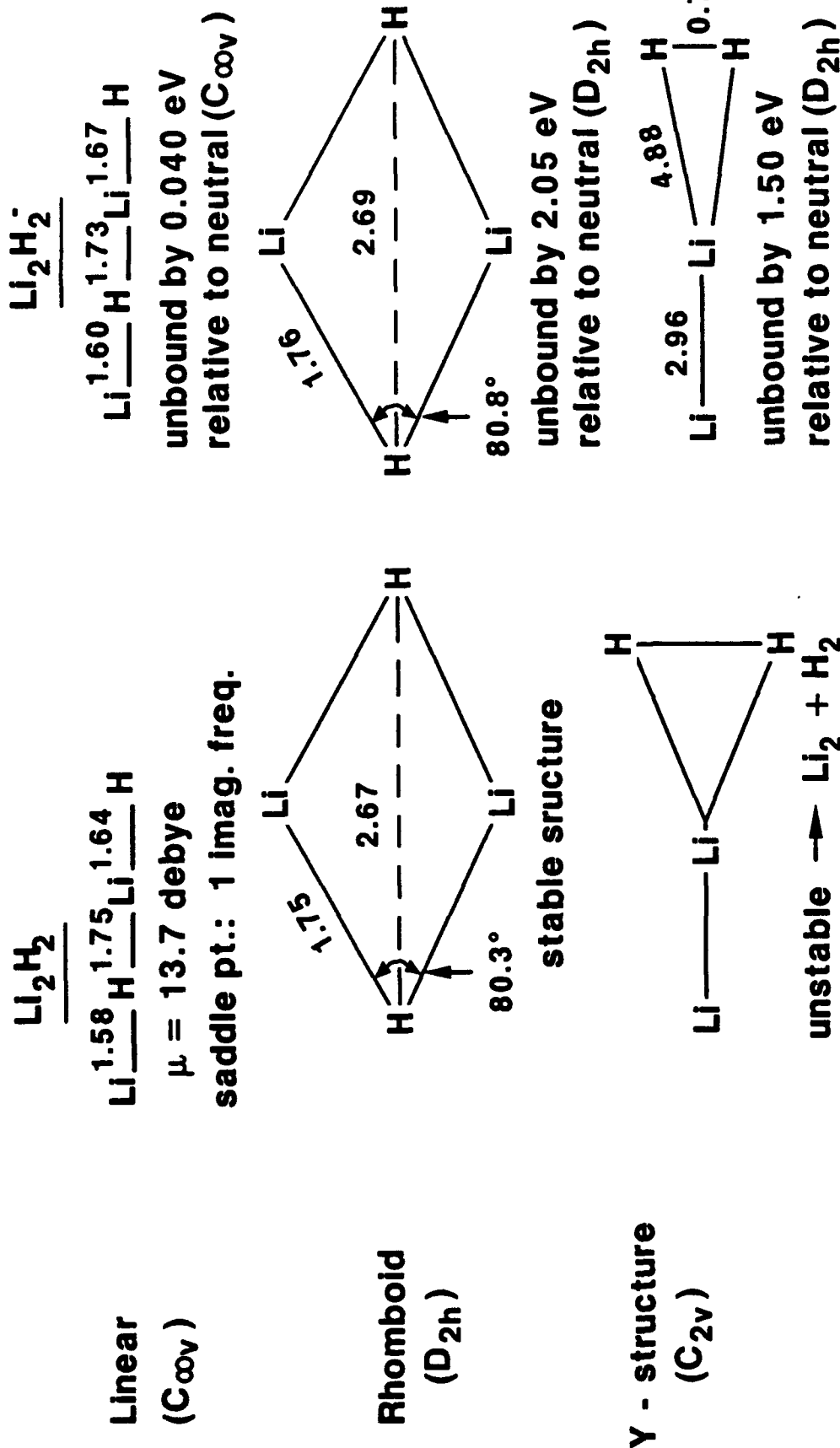
APPENDIX I

ABSTRACTS OF PUBLISHED PAPERS

R92-928101

APPENDIX I-1

POTENTIAL ENERGY CURVES FOR DISSOCIATIVE
RECOMBINATION OF HeH$^+$

H.H. Michels
United Technologies Research Center
East Hartford, Connecticut 06108

ABSTRACT

The potential energy curves pertinent to the process of dissociative recombination (DR) of e + HeH$^+$ have been calculated using an *ab initio* valence configuration interaction (VCI) method. Recombination into both the singlet and triplet ion channels has been considered through analysis of the low–lying doublet and quartet states of HeH. With the exception of the ground state, all of the doublet states up to the HeH$^+$ limit are known to be Rydberg in character. Similarly, we find weak binding for the lowest quartet states of HeH, which appear to be mainly Rydberg to the a$^3\Sigma^+$ state of HeH$^+$. The nature of a second quartet series, which should be Rydberg to the lowest $^3\Pi$ and first excited $^3\Sigma^+$ states of HeH$^+$, is uncertain, owing to possible strong perturbations with the ion–pair states of HeH.

APPENDIX I-2

THEORETICAL STUDY OF IONIZATION AND ELECTRON ATTACHMENT PROCESSES IN RYDBERG ATOM COLLISIONS

H.H. Michels and R. H. Hobbs
United Technologies Research Center
East Hartford, Connecticut 06108

ABSTRACT

Theoretical studies of collisional ionization and electron attachment mechanisms involving light elements (H, He, Li) are being carried out in support of particle beam sources and beam neutralization concepts. In particular, the electronic structure of stable anions, their resonance and metastable states, and radiative and collisional processes describing their formation and/or destruction are being investigated. The volume production of atomic anions via electron–molecule dissociative attachment has previously been examined, both experimentally and theoretically, for $e + H_2$ and $e + Li_2$ collisions. An alternate production route, involving ion–pair formation from Rydberg–Rydberg atom collisions, is currently being investigated. The possible mechanisms include: ionic–Rydberg molecule curve crossings, collisional radiative stabilization, and associative ionization followed by secondary electron–neutral attachment processes. Recent experiments by McGeoch, et al. indicate that associative ionization is highly favored over direct ion–pair production in the Li system. However, both Ciocca, et al and Cheret and Barbier report efficient ion–pair production in collisions between heavier (Na, Rb) alkali Rydberg atoms. Several possible reaction mechanisms have been examined for these systems.

APPENDIX I-3

LASER INDUCED CHEMILUMINESCENCE OF THE LiMg EXCIMER

G. Pichler, A. M. Lyyra, P. D. Kleiber,
W. C. Stwalley, R. Hammer, K. M. Sando
Center for Laser Science and Engineering
University of Iowa
Iowa City, IA 52242 USA

H. H. Michels
United Technologies Research Center
East Hartford, CT 06108

ABSTRACT

A UV Ar^{++} laser was used to excite specific levels in the $C^1\Pi_u$ state of the $^7Li_2$ dimer. A subsequent photochemical reaction with atomic Mg produced the LiMg excimer in excited $C^2\Pi$ and $D^2\Sigma^+$ states. The observed bound–free excimer emission spectrum was compared with theoretical emission profiles based on potential energy curves and transition dipole moments obtained from *ab initio* calculation. These calculations also indicate avoided crossings between the $A^2\Pi$ and $C^2\Pi$ states, and $B^2\Sigma^+$ and $D^2\Sigma^+$ states of LiMg.

APPENDIX I-4

GAS PHASE ALKALI-HYDROGEN INTERACTIONS
IN NEGATIVE ION SOURCES

H.H. Michels
United Technologies Research Center
East Hartford, Connecticut 06108

J. M. Wadehra
Wayne State University
Detroit, MI 48202

ABSTRACT

The role of $Li_xH_y(Cs_xH_y)$ molecules, which can be formed from seeding an alkali into a hydrogen plasma, is examined through *ab initio* calculations of the structure and stability of such species. The simplest alkali hydride, LiH, supports a bound anion for all internuclear separations. Larger structures, such as Li_2H_2 and Li_3H, do not support stable anions but exhibit thermodynamic stability as gas phase molecules. Their possible roles in dissociative attachment to form H^- and/or Li^- is examined.

APPENDIX I-5

DISSOCIATIVE ELECTRON ATTACHMENT TO LIGHT MOLECULES: A COMPARATIVE STUDY OF H_2, LiH AND Li_2

H.H. Michels
United Technologies Research Center
East Hartford, Connecticut 06108

J. M. Wadehra
Department of Physics and Astronomy
Wayne State University
Detroit, MI 48202

ABSTRACT

In this paper we have compared the energetics of three light molecules (H_2, LiH and Li_2) to form negative ions by the process of dissociative electron attachment. For two light homonuclear molecules (H_2 and Li_2) we have done explicit calculations, using the local formalism of the resonance model, to obtain the electron attachment cross sections and the rates of negative ion formation.

APPENDIX I-6

ON THE C-H BOND DISSOCIATION ENERGY OF ACETYLENE

J. A. Montgomery, Jr.
United Technologies Research Center
East Hartford, Connecticut 06108

G. A. Petersson
Hall-Atwater Laboratories of Chemistry
Wesleyan University
Middletown, CT 06457

ABSTRACT

Ab initio calculations, including extrapolation to the complete basis set limit, are reported for the C-H bond dissociation energy of acetylene. These calculations, which have a RMS error of 0.51 kcal/mol per bond for the atomization energies of 13 well-known molecules, give $D_0(H-CCH)$ = 131.54 kcal/mol, in good agreement with previous results, but about 5 kcal/mol above the recent measurement of Green, Kinesey, and Field ($D_0 \leq 126.647 \pm 0.002$ kcal/mol), and that of Segall, Lavi, Wen, and Wittig ($D_0 = 127 \pm 1.5$ kcal/mol). The electron affinity of CCH is calculated to be within 0.18 kcal/mol of the recent measurement of Ervin *et al.* (2.969 ± 0.010 eV).

APPENDIX I-7

STRUCTURE AND STABILITY OF Li_xH_y MOLECULES AND ANIONS

H.H. Michels
United Technologies Research Center
East Hartford, Connecticut 06108

J. M. Wadehra
Wayne State University
Detroit, MI 48202

ABSTRACT

The role of Li_xH_y (Cs_xH_y) molecules, which can be formed from seeding an alkali into a hydrogen plasma, is examined through *ab initio* calculations of the structure and stability of such species. The simplest alkali hydride, LiH, supports a bound anion for all internuclear separations. Larger structures, such as Li_2H_2 and Li_3H, do not support stable anions but exhibit thermodynamic stability as gas phase molecules. Their possible roles in dissociative attachment to form H^- and/or Li^- is examined.

R92-928101

APPENDIX I-8

COMMENT ON "AN EXPERIMENTAL AND THEORETICAL STUDY OF THE NEGATIVELY CHARGED HELIUM DIMER He_2^-

H. H. Michels, R. H. Hobbs
United Technologies Research Center
East Hartford, CT 06108 USA

Y. K. Bae and J. R. Peterson
SRI International
Menlo Park, CA 94025 USA

ABSTRACT

It is shown that the study of the negatively charged helium dimer reported by Krishnamurthy and Mathur contains serious errors in both the theoretical interpretation and experimental analysis of this ion.

APPENDIX I-9

A COMPLETE BASIS SET MODEL CHEMISTRY. III. THE CBS–QCI FAMILY OF METHODS

G. A. Petersson and Thomas G. Tensfeldt
Hall–Atwater Laboratories of Chemistry
Wesleyan University
Middletown, CT 06457

J. A. Montgomery, Jr.
United Technologies Research Center
East Hartford, Connecticut 06108

ABSTRACT

The major source of error in most *ab initio* calculations of molecular energies is the truncation of the one–electron basis set. A family of complete basis set (CBS) quadratic CI (QCI) model chemistries is defined to include corrections for basis set truncations errors. These models are basis sets ranging from the small 6–31G††DZ + P size basis set to the very large (14s9p4d2f,6s3p1d)/[6s6p3d2f,4s2p1d] atomic pair natural orbital basis set. When the calculated energies are compared with the experimental energies of the first–row atoms and ions and the first row–diatomics and hydrides: H_2, LiH, Li_2, CH_4, NH_3, H_2O, HF, LiF, N_2, CO, NO, O_2, and F_2, two very promising new model chemistries emerge. The first is of comparable accuracy, but more than ten times the speed of the G1 model of Pople and co–workers. The second is less than one tenth the speed of the G1 model, but reduces the RMS errors in IP's, EA's, and D_0's to 0.033 eV, 0.013 eV, and 0.53 kcal/mol per bond respectively.

APPENDIX I-10

TEMPERATURE, KINETIC ENERGY, AND ROTATIONAL TEMPERATURE EFFECTS IN REACTIONS INVOLVING ISOTOPES

A. A. Viggiano, R. A. Morris, J. M. Van Doren and J. F. Paulson

Phillips Laboratory, Geophysics Directorate

Ionospheric Effects Division (LID)

Hanscom AFB, MA 01731-5000

H. H. Michels and R. H. Hobbs

United Technologies Research Center

East Hartford, Connecticut 06108

ABSTRACT

Data on four reactions involving isotopes taken in a variable temperature selected ion flow drift tube are presented. A study of the reaction of O^- with N_2O indicates that the reaction proceeds preferentially by bonding of the O^- to the central nitrogen in N_2O. The preference for O^- attack at the central nitrogen over attack at the terminal nitrogen decreases at higher temperatures. In the atom abstraction reaction of O^+ with HD, OH^+ is formed more efficiently than is OD^+ at low temperatures and moderate energy. The branching fraction favoring OH^+ production is also sensitive to the rotational temperature of the HD. The results for this reaction are consistent with a model of the reaction based on the long range part of the ion-neutral potential. Rate constants for the reactions of O^- with H_2, D_2, and HD vary with mass of the hydrogen molecule as predicted from the collision rate constant dependence. These reactions proceed by two channels: hydrogen abstraction and associative electron detachment. The rate constant for the minor hydrogen abstraction channel increases with increasing kinetic energy. The efficiency of the abstraction reaction of O^- with D_2 is significantly smaller than that in the reaction with H_2. More OD^- as compared with OH^- is produced in the reaction of HD. The results are explained by a direct two step mechanism. A large preference for OH^- over OD^- formation in the atom abstraction reaction of O^- with CH_2D_2 is observed. An *ab initio* potential for the reaction path reveals a barrier and indicates that zero point energy effects play a major role in the observed isotope effects. The four reactions studied in this paper, when taken together, show that isotopically labelled reactants can play a major role in elucidating widely different reaction mechanisms.

APPENDIX I-11

VINYLIDENE AND THE HAMMOND POSTULATE

G. A. Petersson and T. G. Tensfeldt
Hall-Atwater Laboratories of Chemistry
Wesleyan University
Middletown, CT 06457

J. A. Montgomery, Jr.
United Technologies Research Center
East Hartford, Connecticut 06108

ABSTRACT

The potential energy barrier for the isomerization of vinylidene, $:C=CH_2$, to acetylene, $HC \equiv CH$, has been calculated by the quadratic configuration interaction method using a 6s6p3d2f,4s2p1d basis of atomic pair natural orbitals with extrapolation to the complete basis set limit (CBS-QCI/[...3d2f] APNO model). The calculated barrier ($\Delta E_c^{\ddagger} = 2.2 \pm 0.5$ kcal/mol) and energy change from vinylidene to acetylene ($\Delta E_o = -43.9 \pm 0.5$ kcal/mol) are in excellent agreement with recent experimental values ($\Delta E_c^{\ddagger} = 2$ kcal/mol, and $\Delta E_o = -43 \pm 2$ kcal/mol). In spite of the small barrier height for this strongly exothermic reaction, the transition state is located halfway between the reactant and product in apparent violation of the Hammond postulate. The potential energy surface for the isomerization can best be understood by considering two distinct processes. The location of the transition state is determined by the hydrogen migration which has a significant barrier, whereas the exothermicity results from the conversion of the lone pair of vinylidene to a π bond in acetylene. Each of these processes individually satisfies the Hammond postulate.